5-1-2008

Transitional Flow Between Orifice and Non-Orifice Regimes at a Rectangular Canal Gate

Omar Alminagorta Cabezas
Utah State University

TRANSITIONAL FLOW BETWEEN ORIFICE AND NON-ORIFICE REGIMES

AT A RECTANGULAR CANAL GATE

by

Omar Alminagorta Cabezas

A thesis submitted in partial fulfillment
of the requirements for the degree
of

MASTER OF SCIENCE

in

Irrigation Engineering

Approved:

Gary P. Merkley Committee Chair	Gilberto Urroz Committee Member
Wynn R. Walker Committee Member	Byron R. Burnham Dean of Graduate Studies

UTAH STATE UNIVERSITY
Logan, Utah

2008

ABSTRACT

Transitional Flow Between Orifice and Non-Orifice Regimes

at a Rectangular Canal Gate

by

Omar Alminagorta Cabezas, Master of Science

Utah State University, 2008

Major Professor: Gary P. Merkley
Department: Irrigation Engineering

The main objective of this research was to analyze the hydraulic transition between non-orifice and orifice flow regimes at a rectangular sluice gate through the calibration of various discharge equations, and determining the value of a coefficient, which defines the transition between orifice and non-orifice flow conditions. The second objective was to determine whether a single equation could be used to represent the stage-discharge relationship for both free and submerged non-orifice flow through a rectangular sluice gate.

Several hundred data sets were collected in a hydraulic laboratory, each including the measurement of water upstream depth and downstream for five different gate openings, and 17 different steady-state discharges, from 0.02 to 0.166 m^3/s. Three approaches were used to define the limits of the non-orifice-to-orifice regime transition: (1) using an empirical equation; (2) using the traditional submerged non-orifice equation; and (3) using the specific-energy equation for open-channel flow. Based on the results of this research, the latter approach was ultimately chosen to define the boundaries of the transition between orifice and non-orifice flow regimes.

Once the transition limits were defined, the estimation of the non-orifice-to-orifice transition coefficient, C_o, was made. The transition coefficient was defined as the ratio of gate opening to upstream water depth. The experimental results indicate that orifice flow always exists when C_o is less than 0.83, and non-orifice flow always exists when C_o is greater than 1.00. To identify the flow regime (orifice or non-orifice) within the range $0.83 < C_o < 1.00$, it is necessary to consider the submergence, S, which is the ratio of downstream to upstream water depth.

With respect to the second objective, laboratory data for non-orifice flow regimes were used to test several different empirical equation forms that could potentially represent both free and submerged flow conditions. The strategy was to find a relationship among flow rate, upstream depth, downstream depth, and submergence. As a result of the analysis, one particular equation form was found to have a relatively high coefficient of determination and low standard error of the estimate. This equation fits the laboratory data for submergences up to 0.87 with a discharge error not exceeding ±10%.

(93 pages)

ACKNOWLEDGMENTS

I would like to sincerely thank to my advisor, Dr. Gary Merkley, for his guidance and support in this thesis. His patience and advice were greatly appreciated. I would also like to thank to the committee members, Drs. Wynn R. Walker and Gilberto Urroz, for their constructive suggestions. Additionally, I want to thank Dr. Robert W. Hill for his cooperation and assistance.

I am grateful to my entire family for their loving support and encouragement during this time of my life, with special thanks to Máximo, Eladio, and Julia, without whom this work would never have come to fruition, and to whom I dedicate this study.

I would like to express my appreciation to Jorge Escurra Cabrera and his family, who motivated me to study abroad and helped me throughout my studies. Finally, this list of appreciation could not be concluded without recognizing the support of my friends at USU, with special thanks to Alfonso Torres.

Omar Alminagorta

CONTENTS

LIST OF TABLES

LIST OF FIGURES

LIST OF SYMBOLS

b	flume width (m);
C_o	transition coefficient;
E_d	specific energy at the downstream tap (m);
E_u	specific energy at the upstream tap (m);
G_o	vertical gate opening (m);
G_w	gate throat width (m);
h_d	piezometric head at the downstream tap (m);
h_u	piezometric head at the upstream tap (m);
h_{NOt}	piezometric head at the upstream non-orifice threshold condition (m);
h_{Ot}	piezometric head at the upstream orifice threshold condition (m);
n_f	free-flow exponent;
n_s	submerged-flow exponent;
n_{s1}	submerged-flow numerator exponent;
n_{s2}	submerged-flow denominator exponent;
Q	flow rate (m^3/s);
r^2	coefficient of determination;
R_e	Reynolds number;
S	submergence (h_d/h_u);
S_g	specific gravity of a fluid;
S_t	transition submergence; and,
SEE	standard error of the estimate.

CHAPTER I

INTRODUCTION

Definition of the Problem

Gates are commonly used to control and measure flow rates in irrigation canals, water treatment plants, hydroelectric power plants and flood control among other structures. Gates offer significant advantages over many conventional structures; they are easy to operate, inexpensive and have relatively low head loss. These advantages over other structures make them that used in many projects.

Flow under a sluice gate and calibrations of sluice gates are classic problems in hydraulics, but despite numerous research studies, discharge calibration accuracy for these structures for non-orifice flow has not been adequate for water management purposes. Yet, non-orifice conditions at a sluice gate are commonly observed in practice and represent a significant obstacle to flow measurement capability when the relationship between water depth(s) and flow rate is not accurately known. Thus, it would be of great value in water management and canal operations to have the capability to use sluice gates for flow measurement under any flow regime.

Four types of flow can be observed in steady-state conditions in a gate: free- and submerged-flow, orifice and non-orifice flow, in which each has a unique equation and the flow can transit from any regime to another, the changes between some of the flow regimes usually involve flow rate discontinuities. These situations can provoke problems during the control and measurement of flow rates. Calibration of these gates has been difficult, especially in the transition zone, where the flow changes from orifice to non-orifice, or from free- to submerged-flow. Equations developed for these flow regimes work very well in defined flow conditions but not for transition or submerged-flow.

The identification of the flow regime is crucial to determine the correct equation to apply. Thus, the necessity to improve flow measurement through sluice gates has driven the development of further research, focusing on the definition of the different flow regimes that can occur through gates. However, little published information can be found about the determination of the condition when non-orifice flow becomes orifice flow, and vice versa. The intent of this research was to contribute to the solution of this problem by determining the coefficient which defines the transition from orifice to non-orifice flow, and to determine whether a single equation can be used for free and submerged non-orifice flow through a gate.

Research Objectives

The main objective of the proposed research is to analyze the parameters related to water measurement through a rectangular gate. The specific objectives of the research were:

1. To measure water depths and flow rates through a vertical rectangular gate in a hydraulic laboratory, and to make detailed observations of the transition between orifice and non-orifice regimes at different steady-state discharges for free- and submerged-flow conditions;
2. To measure water depths and flow rates through the same vertical rectangular gate in a hydraulic laboratory, and to make detailed measurements of upstream depth, h_u, and submergence (h_d/h_u) at different steady-state discharges, starting with free flow and transitioning gradually to submerged-flow conditions;
3. To analyze the laboratory data for the calibration of the various discharge equations, to determine the value of the coefficient which defines the transition from orifice to non-orifice flow, and to determine whether a single equation can be used for free and submerged non-orifice flow through the gate; and,
4. To make recommendations about the application of the free- and submerged-flow equations for flow measurement in vertical rectangular canal gates.

CHAPTER II

LITERATURE REVIEW

Gates are structures, which control flow rate and upstream water surface elevation, that can also be used for flow measurement purposes (Ames 1999). These structures can operate under at least four different flow regimes, as described in the following.

Flow Regime Changes at a Gate Structure

The type of flow regime is a function of discharge and gate opening. Flow changes can be induced by varying upstream or downstream discharge, as well by routine gate operation (Hadi 2003). In general, four kinds of flows can be observed at the gate, each of the four regimes has a unique equation, and flow can transition from any regime to the other (Merkley 2006a). Figure 1 and Table 1 show the four possible flow regimes at a vertical sluice gate structure: free orifice (FO); submerged orifice (SO); free non-orifice (FN); and, submerged non-orifice (SN).

	Free	**Submerged**
Non- Orifice	FN	SN
Orifice	FO	SO

Fig. 1. Four type of flow conditions at a gate structure

Conditions where the equations are of typically low accuracy are in the transition zone from free to highly submerged flow, and sites where the downstream channel is much wider than the gate chamber (Wahl 2004).

In this research, the concepts of submergence and Froude number were applied. Submergence is defined as the ratio of downstream to upstream water depth at a structure and is expressed as follows:

$$S = \frac{h_d}{h_u} \qquad (5)$$

Table 1. Four Possible Flow Regimes at a Gate Structure (Merkley 2006)

Flow Condition	Characteristic	Equation	Side view of a Gate
1. Free non-orifice (FN)	Defined as flow free non-orifice, when the gate bottom is above the water surface and the flow is not affected by water condition downstream.	$F_{FN} = Q_f - C_{df} h_u^{n_f} = 0$ (1)	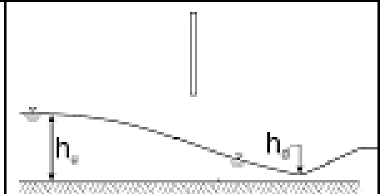
2. Submerged non-orifice (SN)	Defined as flow submerged non-orifice, when the gate bottom is above the water surface and the flow is affected by water condition downstream.	$F_{SN} = Q_s - \frac{C_{df}(h_u - h_d)^{n_f}}{(-\log_{10} S)^{n_s}} = 0$ (2)	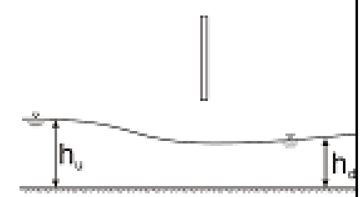
3. Free orifice (FO)	Defined as flow under a gate, when the issuing jet of supercritical flow is open to the atmosphere.	$F_{FO} = Q_f - C_{df} A \sqrt{2g(h_u - C_c G_o)} = 0$ (3)	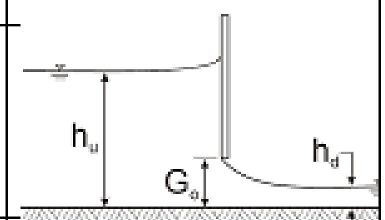
4. Submerged orifice (SO)	Defined as flow under a gate, when the jet of water flowing under the gate is submerged.	$F_{SO} = Q_s - C_{ds} A \sqrt{2g(h_u - h_d)} = 0$ (4)	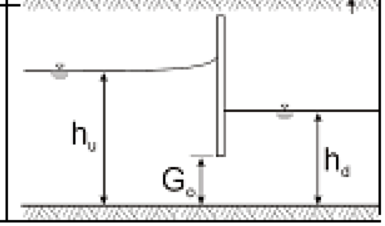

where Q is flow rate (discharge); A is the area of the orifice structure opening; h_u is the upstream depth; h_d is the downstream depth; G_o is the vertical gate opening; S is submergence (h_d/h_u); g is the ratio of weight to mass; and the other terms are calibration parameters.

where S is submergence; h_d is downstream depth (m); and, h_u is upstream depth (m).

The Froude number is the ratio of the velocity in an open channel to the speed of propagation, or celerity, of a small amplitude gravity wave (Jeppson 2001):

$$F_r = \frac{V}{c} = \frac{V}{\sqrt{\frac{gA}{T}}} = \sqrt{\frac{Q^2 T}{g^* A^3}} \quad (6)$$

where F_r is the Froude number; V is velocity (m/s); c is a small amplitude gravity wave; Q is flow rate (m^3/s); T is width of the water surface (m); and A is cross-sectional area (m^2).

Previous Work

The necessity to improve flow measurement through gates structures has been the impetus for the development of new research on the hydraulics of vertical sluice gates. Previous work in this area in recent years includes the hydraulic analysis of a gate structure (Nguyen 2000), radial gate calibration (Clemmens et al. 2003), and the development of a single equation for free and submerged flow in a Cutthroat flume (Torres 2006).

Nguyen (2000) provided a preliminary study about the transition regime at the gate and report that the main cause of numerical instability in a mathematical model for simulating flow regimes at a gate is the discharge discontinuity at the transitional flow regime. Thus, this regime should be studied more carefully. Nguyen reported a constriction coefficient, defined as a ratio between the water depth at the gate and the upstream gate to free and submerged non-orifice. From the laboratory data, taken during his research using a rectangular sluice gate with a gate width of 0.217 m and a channel width of 0.298 m, he reported values of constriction coefficient from 0.90 to 0.98 for free non-orifice flow, and from 0.92 to 0.98 for submerged non-orifice flow. He concluded that constriction coefficient could be used to calculate water depth at a gate instead of the gate opening, G_o, for orifice flow conditions.

Research by Clemmens et al. (2003) led to the development of a calibration for radial gates. Clemmens, used a method for free-flowing and submerged radial gates. The method uses the energy equation on the upstream side of the structure and the momentum equation on the downstream side, thus is called the energy-momentum method. An iterative solution is required to solve these two equations, allowing calibration from free flow to submerged flow continuously through the transition.

A study related to determined whether a single equation can be used for free and submerged flow in a Cutthroat was established by Torres (2006). He determined that a single equation (Eq. 7) can be used for free and submerged non-orifice flow through a channel constriction. Torres (2006) made a series of calibrations of existing free- and submerged-flow equations based on the analysis of laboratory data, calculating the transition submergence values and compared with previously published transition submergence values. These equations were calibrated to determine the accuracy of the equation to describe the data.

$$h_u = h_{uf} + \left(\frac{aQ + b}{\left[\ln \left(cQ + dS^e \right) \right]^f} \right) \tag{7}$$

where Q is the flow rate; h_u is the measured upstream water depth; h_{uf} is the upstream water depth for free-flow conditions; the letters a, b, c, d, e, and f represent fitted equation parameters; and, S is submergence. The units of Q and h_u are typically m^3/s and m, or cfs and ft, respectively.

The threshold between free- and submerged-flow non-orifice conditions at the gate is the transition submergence, S_t, which can be defined by equating the free-flow (Eq.1) and submerged-flow (Eq. 2) discharge equations. As a result, if the actual submergence is less than S_t, the free-flow equation is used; otherwise the submerged-flow equation is applied. However, this procedure often produces multiple, different S_t values, causing inaccuracies in the application of the traditional equations. Thus, there is a necessity to investigate the possibility of using a single equation for both free and submerged non-orifice flow regimes, instead of two separate equations.

Transition Coefficient, C_o, for Non-Orifice and Orifice Flow Regimes, and Contraction Coefficient, C_c

The use of C_o or C_c can sometimes be ambiguous. For this reason, it is important to define these parameters. The contraction coefficient, C_c takes the ratio between water depth at the contraction location, h_c, and the vertical opening of the gate (G_o). In contrast, C_o is the ratio between vertical gate opening, G_o,and upstream depth, h_u. In Fig. 2 it is seen that the contraction coefficient is defined as $C_c = h_c/G_o$ and $C_o = G_o/h_u$.

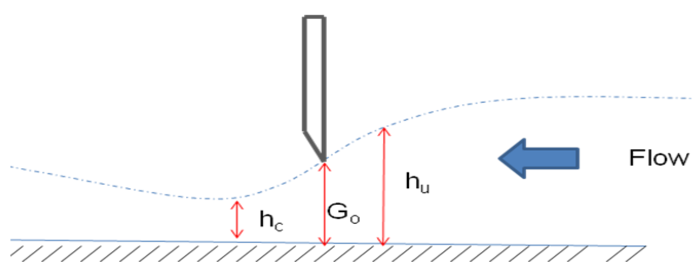

Fig. 2. Side view sketch of a vertical sluice gate in an open channel

Merkley (2006a) defines C_o as a coefficient to determine the transition between orifice and non-orifice flow regimes. This coefficient is compared with the gate setting to define the flow regime.

$$C_O \, h_u \leq G_O \tag{8}$$

Equation 8 implies that there is insufficient upstream hydraulic seal (non-orifice), whereas the following equation is for orifice conditions:

$$C_O h_u > G_O \tag{9}$$

where C_o is a coefficient to determine the transition between orifice and non-orifice regimes; G_o is the gate opening; and, h_u is the depth of water on the upstream side of the gate. Merkley (2006a) reported a range of C_o from 0.80 to 0.99.

CHAPTER III

EXPERIMENTAL DESIGN

The data were collected at the Utah Water Research Laboratory (UWRL) at Utah State University. A sluice gate was designed, constructed and installed in a rectangular flume. Flow depths upstream and downstream were measured using water manometer to analyze the different flow regimes.

Description of the Flume and Rectangular Gate

The rectangular flume that was used in this research consists of a steel frame with transparent acrylic panels. It is 7.26 m in length, 0.93 m wide and 0.61 m deep, with a longitudinal bed slope of 0.24%. The flume receives water through two pipes: 0.10 m and 0.30 m (nominal diameters). Both water supply pipes included sharp-edged, circular orifice plates to measure the discharge entering the rectangular flume during operation. The details of flume and the location of the gate in the flume can be observed in Fig. 3.

The flume has a manually adjustable tailgate, located at the downstream end of the rectangular flume. The tail gate is hinged on the channel floor and measures 0.3 m in length, and 0.93 m in width, similar to the cross-sectional dimensions of the rectangular flume. The tail gate can be adjusted by tightening or loosening a wing nut attached to a threaded rod which extends to the downstream end of the gate (Fig. 4).

Water Manometer

The flume includes four piezometer taps located at the right sidewall (upstream and downstream). The upstream piezometer taps were located in an attempt to avoid the regions of significant water surface drawdown. The downstream piezometer taps were located such that the downstream hydraulic jump, when it is manifested, is beyond the taps. The details of the tap locations can be observed in Fig. 5.

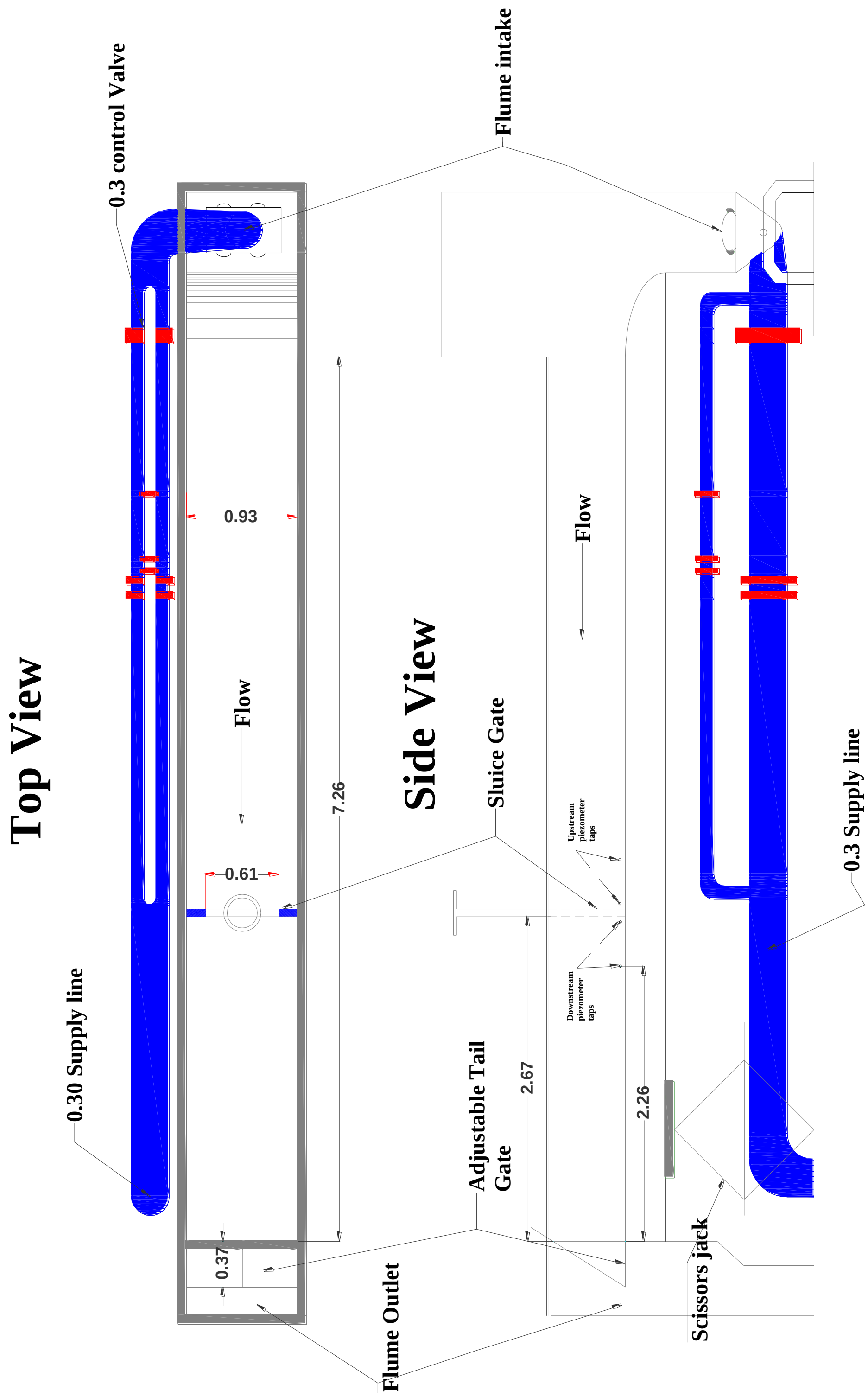

Fig. 3. Top and side views of the 0.93 m rectangular flume

Fig. 4. Photograph of the downstream of the flume with a tailgate to control the water depth downstream of the sluice gate

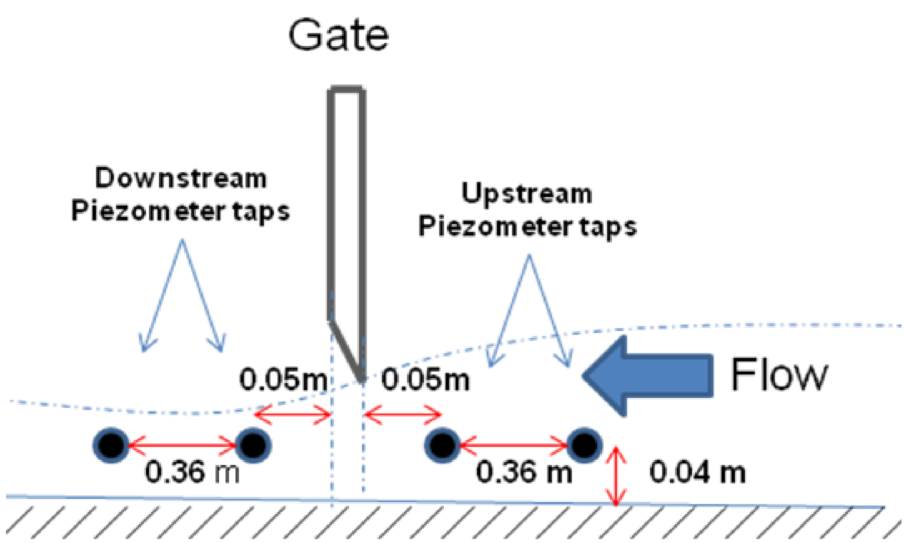

Fig. 5. Side view of the flume, showing the locations of the taps

The piezometric head at each tap was measured on a water-based manometer board that was attached to the outside of the rectangular flume (see Fig. 6). Plastic tubes with 0.5-cm inside diameter were installed from the taps to the manometer board. The manometer board has a range from 0 to 40 cm on a metallic gauge with marks at 0.1-cm intervals, and it was used to measured the upstream and downstream depths.

Fig. 6. Rectangular flume, sluice gate, and manometer board

Gate Description

A sluice gate was designed and fabricated, then installed at a distance of two-thirds of the total flume length from the upstream end of the flume, which is consistent with the experimental design by Nguyen (2000). The gate had a steel frame with clear acrylic panels, with a maximum opening area of 0.61 m wide by 0.61 m high. The frame included a 5-mm thick metal base, which was bolted to the rectangular flume's floor. The flap gate was rectangular and was operated using a hand wheel. Figure 7 shows a photograph of the gate, and details of its designed and construction can be found in Appendix I. The gate had an upstream face flat and with an angle of 45° bevel at the gate lip (bottom edge). The gate width was designed to be smaller than the flume width to simulate typical gate installations in the field.

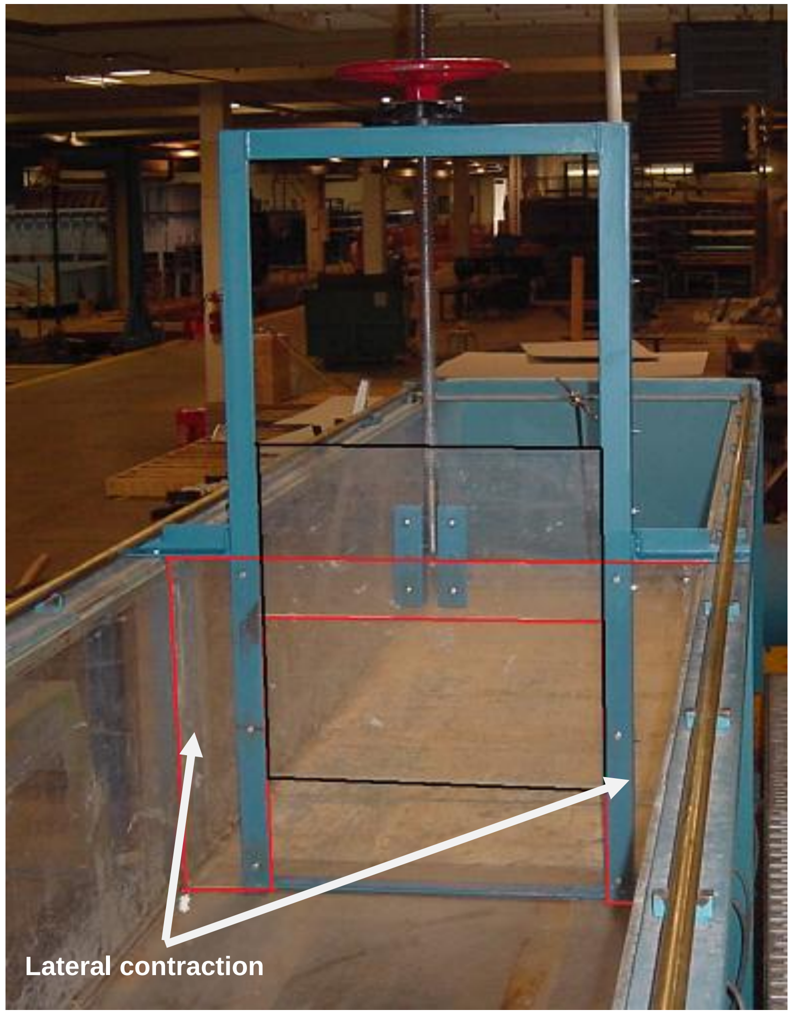

Fig. 7. Photograph of the gate structure showing the lateral contraction in the flume

Flume Inflow Measurement

To measure the discharge entering in the flume during operation, upstream and downstream taps were connected by small hoses to two different manometers which measure the head differential across the respective orifice plates. One of the manometers used mercury for high discharges, and the other used a lower-density fluid called informally used “blue” for smaller discharges.

The accuracy of the orifice plates was approximately ±0.25 to ±0.50% of the actual flow rate in the pipes, according to the UWRL technical staff. The steady-state discharge was calculated using Eq. 10 (Miller 1996):

$$Q = C_d \, A_t \, \frac{\sqrt{2g(h-(S_g-1)}}{\sqrt{1-\left(\frac{D_o}{D_i}\right)^4}} \tag{10}$$

where A_t is the cross-sectional area of the orifice plate opening (m^2); h is the change in piezometric head across the orifice (m); D_o is the diameter of the circular orifice opening (m); D_i is the inside diameter of the upstream pipe (m); h is the measured change of height of the fluid used in the manometer (m); S_g is the specific gravity of the manometer fluid (1.75 for the blue and 13.6 for mercury); and C_d is a dimensionless orifice discharge coefficient, as calibrated by UWRL staff (Torres 2006). Appendix II shows the details of the equation used to calculate discharge past the orifice plates.

Experimental Procedure

Data Collection

This experiment was conducted in a rectangular flume as described above. The longitudinal bed slope was measured in the flume to determine and leveled to 0.24 % of slope in the longitudinal directions. Five different gate openings (0.15, 0.20, 0.25, 0.30, 0.35 m) and 17 different discharges were used. Each series of measurements included the following steps:

1) Set the vertical gate opening.
2) Set the tail gate in the completely lowered (horizontal) position to provide free-flow conditions at the rectangular sluice gate.
3) Establish a constant flow rate in the flume using a supply pipe with a nominal diameter of 0.305 m. Manometer readings using either “blue” or mercury (as appropriate, depending on the flow rate) were taken to determine the discharge.

4) Take measurements of h_u and h_d at four locations: two upstream and two downstream of the gate. Each set of measurements was taken after observing that steady-state conditions had been reached, and after successfully evacuating all air bubbles from the plastic tubes, which were connected, to the water manometer.
5) Record observations (e.g. orifice or non-orifice, occurrence of hydraulic seal, occurrence of a hydraulic jump, and others). Take short video clips and photographs, as necessary, for documenting various hydraulic phenomena.
6) Raise the tail gate a small amount and repeat steps 4 to 6. Figure 8 presents part of the methodology used in the data collection.

This data collection process was continued for a given fixed flow rate. A sample data sheet is shown in Appendix III. The incremental changes in tail gate setting were small enough to provide different submergence values (h_d/h_u). Special attention was given near the transition from non-orifice to orifice; thus, smaller increments in the tail gate were made when it was observed that the flow regime was in transition.

After completing the measurements for a selected discharge, the flow rate was increased and the procedure from steps two to six (see above) were repeated. This was continued until the required measurements for different discharges and five different vertical gate openings.

Water temperature measurements were periodically taken for calculation of the Reynolds number and determining the discharge through the orifice plate in the supply pipe. And, as indicated above, all measurements were taken under steady-state flow conditions. Thus, after a change in the tail gate position, discharge, or gate opening, a waiting period of ten minutes (in the majority cases) was necessary to ensure steady-state hydraulic conditions.

Two water depths were measured upstream of the gate, and two other depths were measured downstream of the gate, for each of the several flow conditions. Upstream and downstream measurements closest to the gate are referred to as the “inner” depth values, and the other pair of upstream and downstream depths were the “outer” values. However, the data analysis presented herein only considers the upstream and downstream depth measurements nearest to the gate (i.e. the inner values). This is because there was usually a hydraulic jump at the “outer” downstream tap location, and it was difficult to obtain accurate readings due to the fluctuations of the water depth at that location.

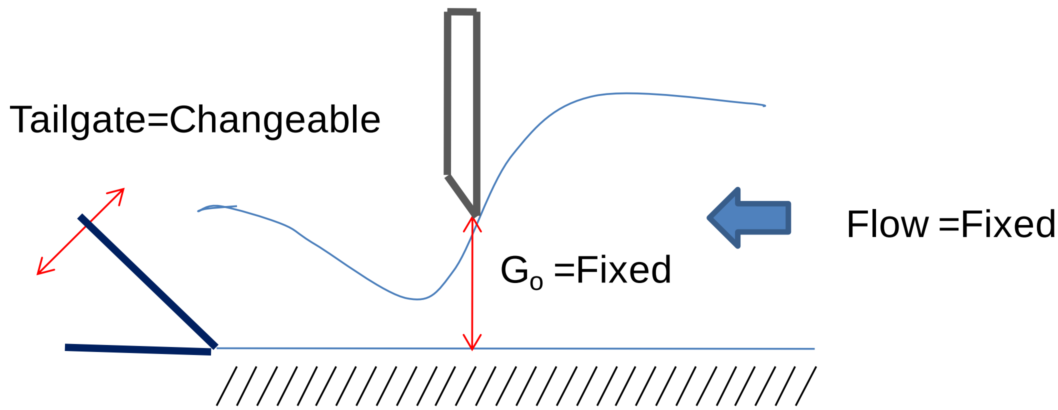

Fig. 8. Side view of the rectangular flume showing part of the methodology used

Data Analysis

With all of the information generated by the data collection procedure, the data analysis consisted of the following:

1. Study the relationship among the transition submergence, piezometer readings, and discharge using statistical tools;
2. Define the transition limits between non-orifice and orifice flow;
3. Calculate the range of the transition coefficient, C_o; and,
4. Determine whether a single equation could be used for free and submerged non-orifice flow through the gate.

CHAPTER IV

RESULTS

There are three main parts to this chapter. The first provides general information about the data collection. The second part deals with the analysis of the transition from orifice to non-orifice flow, determining the value of the coefficient, which defines the transition. Finally, there is documentation of the efforts to define a single calibration equation, which can be used for both free and submerged non-orifice flow through a rectangular sluice gate. The information used in the analysis was the data obtained from the laboratory procedure, as described in Chapter III.

General Information

Description of the Laboratory Data

In order to describe the behavior of the different flow conditions (non-orifice, transition, and orifice) a total of 712 data sets were collected in the laboratory. Each data set consisted of measurements of upstream and downstream water depths, h_u and h_d, for 17 different discharges and five vertical gate openings, G_o. The discharges used for each gate opening are presented in Table 2; for example, with G_o = 0.15 m, a range of flow rates from 0.020 m^3/s to 0.066 m^3/s was used.

Considerations to Distinguish Among Flow Regimes Through a Gate

Since the gate has different flow regimes, the collected data were distinguished in non-orifice (free-submerged), transitional and orifice flow, the Froude number, F_r, at the downstream gate was the criterion used to distinguish the change of flow regimes between free and submerged for non-orifice. Figure 9 shows how the laboratory data were categorized.

Table 2. Data Collected in the Laboratory with Different Discharge and Vertical Gate Opening

Flow Rate (m^3/s)	Vertical Gate Opening , Go (m)				
	0.15	0.20	0.25	0.30	0.35
0.020	X	X			
0.027	X		X	X	X
0.035	X	X	X	X	
0.045	X	X			
0.046	X	X	X	X	X
0.051	X	X	X	X	X
0.055	X	X			
0.058	X	X			
0.066	X		X	X	X
0.075		X	X	X	X
0.082		X			
0.091			X		
0.100		X	X		
0.100			X	X	X
0.117			X	X	X
0.135			X	X	X
0.151				X	X
0.166				X	X
Number of Flows	9	10	11	11	10

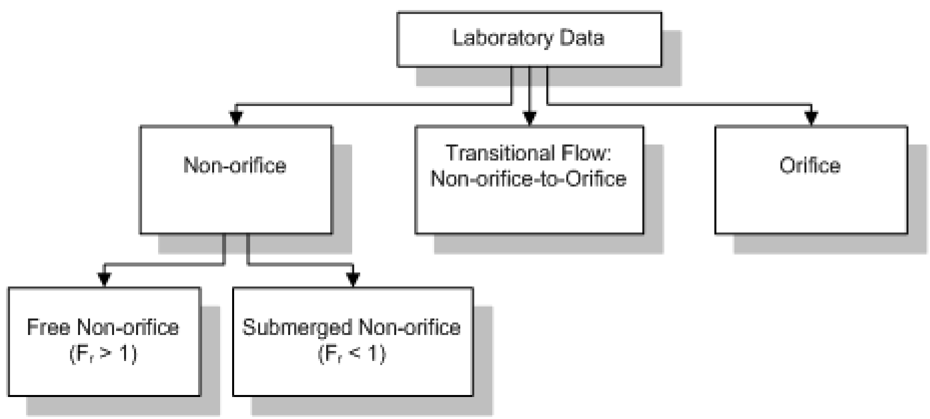

Fig. 9. Flowchart indicating how data were distinguished in different regimes, and the criterion used to differentiate the data

Considerations to Distinguish Between Non- Orifice and Orifice Flow Regimes

To obtain data for non-orifice flow regimes at the sluice gate, the gate was completely raised, ensuring that the lip (bottom edge) of the gate was out of the water. In total of 292 points for non-orifice flow conditions were collected, considering the sum of data non-orifice free and submerged conditions. The criterion for distinguishing orifice flow as orifice was taken from Nguyen (2000) as the condition "when the total of the gate opening is higher than water depth at the gate." In other words, orifice conditions occur when the upstream depth is sufficient to seal the gate. Therefore, the upstream hydraulic seal was checked visually, and it was determined that a total of 326 data points corresponded to an orifice flow regime.

Considerations to Distinguish Between Free and Submerged Non-Orifice Flow Regimes

Free flow for the non-orifice regime is a condition where the flow through gate is not affected by the tail-water and the flow is governed only by the upstream water conditions. This flow condition corresponds to all data with $F_r > 1$ (supercritical flow) downstream of the sluice gate. Most of the points that were taken with the tail gate in fully-open corresponding to the condition free non-orifice and it is usually the presence of hydraulic jump as shown in Fig. 10. A total of 51 data sets were collected for the free non-orifice regime through the sluice gate.

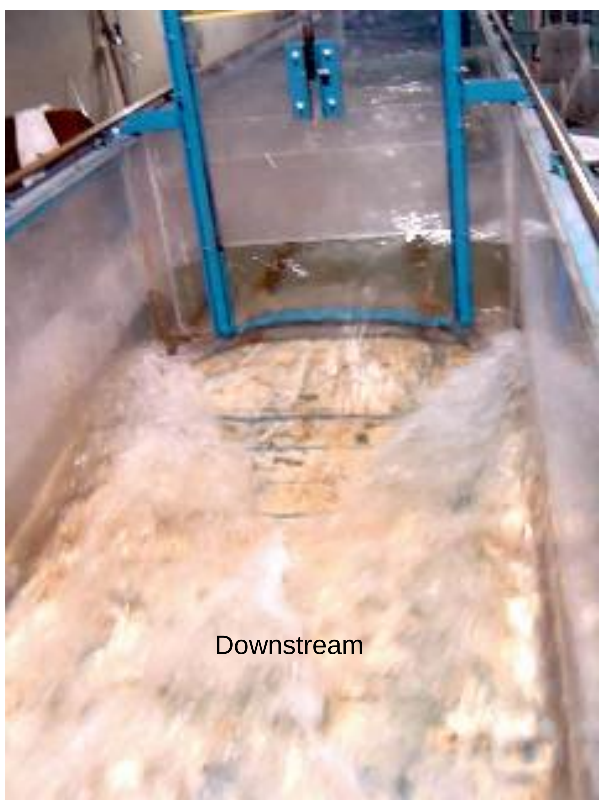

Fig. 10. Laboratory photograph showing an example of a free non-orifice flow regime

Submerged non-orifice flow is a condition whereby the flow through the gate is affected by the existence of tail-water, and the gate is up out of water (not touching the water surface). In this condition, the flow is governed by both upstream and downstream hydraulic conditions. This flow condition corresponds to all data with $F_r < 1.0$ (subcritical flow, as shown in Fig 11) downstream of the sluice gate. In total, 241 points were taken for submerged non-orifice flow conditions.

Fig. 11. Laboratory photograph showing an example of a submerged non-orifice flow regime

Description of the Laboratory Data

Figures 12 to 16 show the variation of upstream depth, h_u, and submergence, S, for each gate opening, G_o, and for different flow conditions (free and submerged non-orifice and orifice). The data used in these figures are found in Appendix IV. Some common characteristics related to the data shown in each figure are as follows:

- Each curve corresponds to a fixed and unique steady-state discharge. The "curves" are actually straight lines connecting adjacent data points;
- Preliminary boundary between non-orifice and orifice is shown in dashed line, orifice flow exist above the dashed line and non-orifice flow below the dashed line;
- The boundary among non-orifice, orifice free and submerged-flow conditions is different for each curve; and,
- The non-orifice part of curve shows lower change of h_u for any submergence. In comparison with the concave curve of orifice, where the h_u value increases as a function of the submergence.

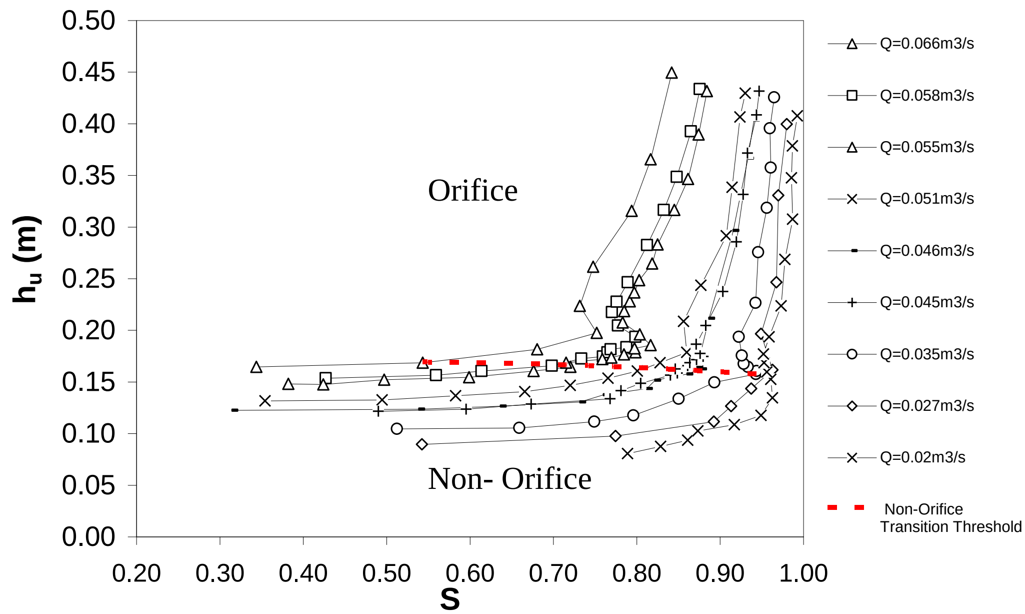

Fig. 12. Upstream water depth (h_u) vs. submergence (S) for G_o = 0.15 m, where orifice flow exists above the dashed line and non-orifice flow below the dashed line

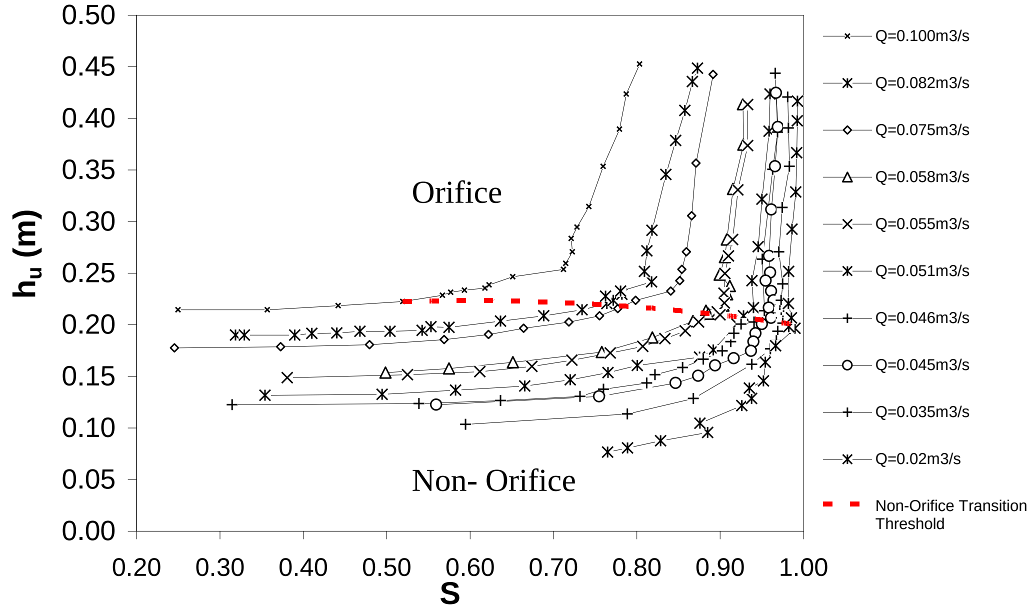

Fig. 13. Upstream water depth (h_u) vs. submergence (S) for G_o = 0.20 m, where orifice flow exists above the dashed line, and non-orifice flow below the dashed line

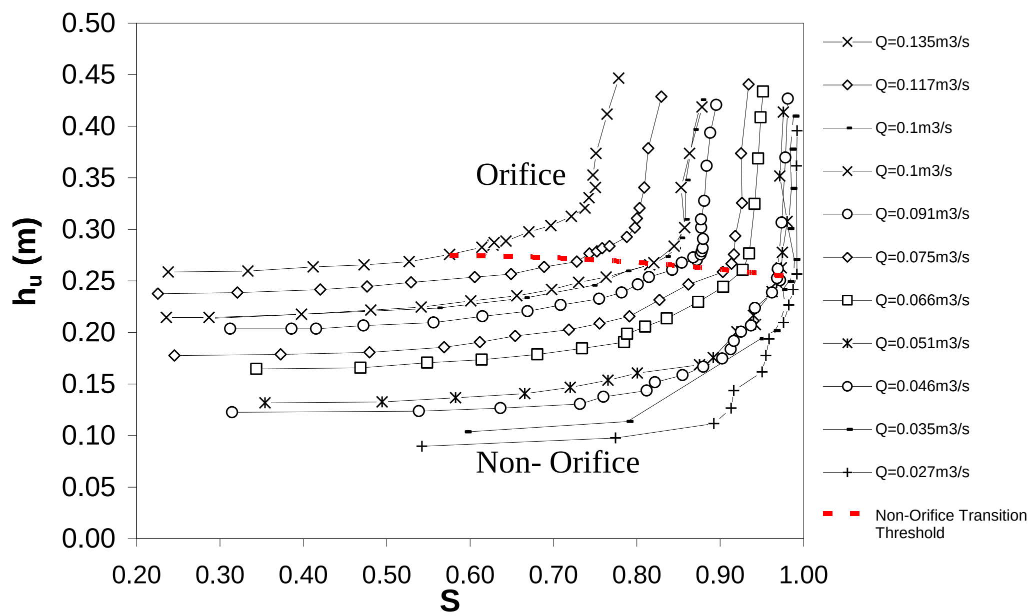

Fig. 14. Upstream water depth (h_u) vs. submergence (S) for G_o = 0.25 m, where orifice flow exists above the dashed line, and non-orifice flow below the dashed line

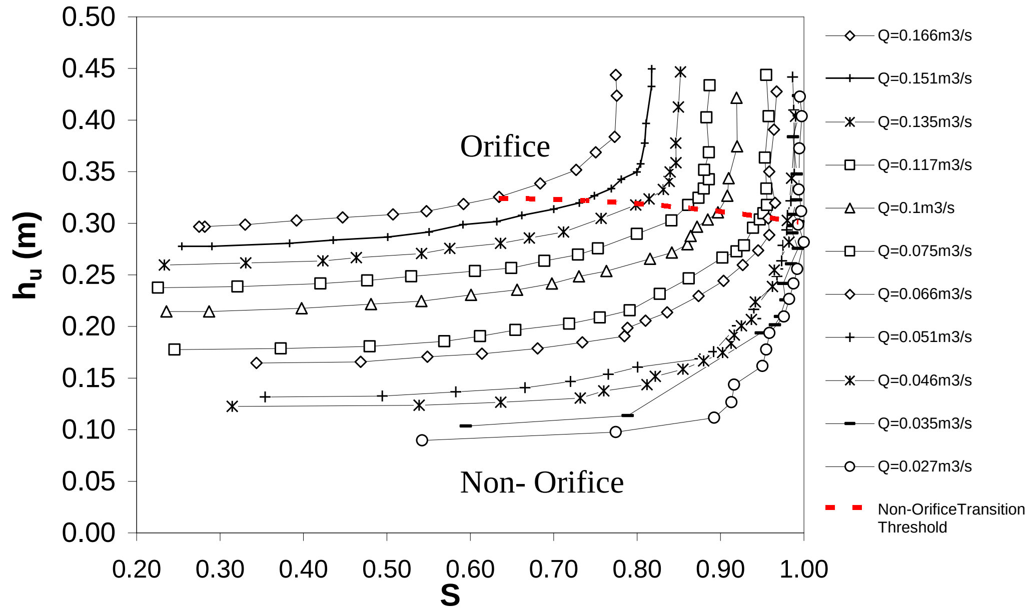

Fig. 15. Upstream water depth (h_u) vs. submergence (S) for G_o = 0.30 m, where orifice flow exists above the dashed line, and non-orifice flow below the dashed line

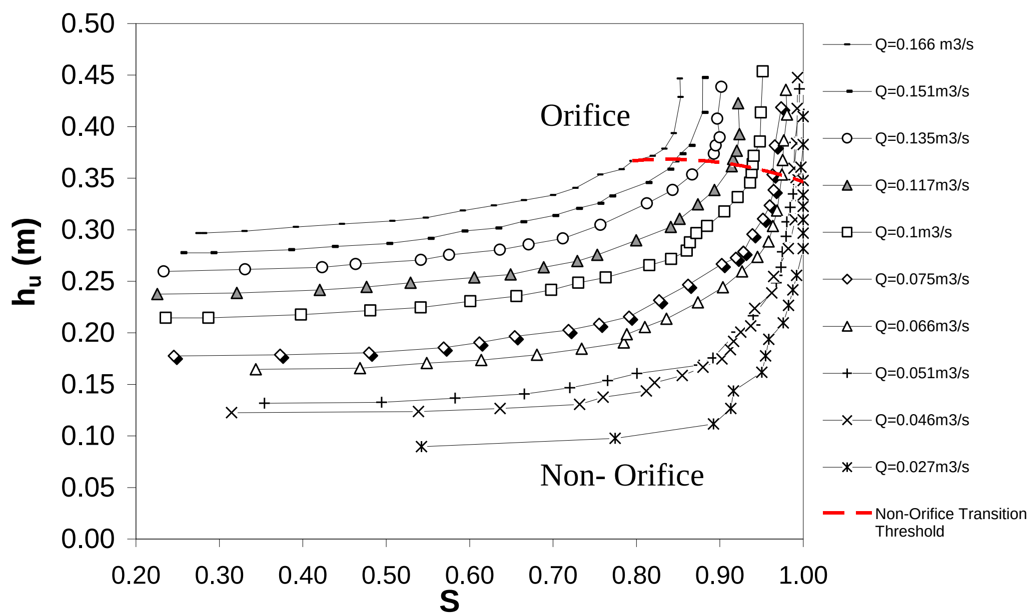

Fig. 16. Upstream water depth (h_u) vs. submergence (S) for G_o = 0.35 m, where orifice flow exists above the dashed line, and non-orifice flow below the dashed line

The following three general conclusions can be made from the analysis of Figs. 12, 13, 14, 15, and 16:

- Each curve is composed of three or four sub-curves: (1) an initial curved line which corresponds to the free-flow non-orifice condition; (2) a straight line which is related to the submerged-flow non orifice condition (the dashed line represent the first condition, where the flow is affected by the lips of the gate); (3) free-flow orifice condition (may only appear at higher discharges, greater than 0.1 m^3/s); and (4) submerged orifice condition, where the submergence values are highest.
- Low-discharge curves have shapes, which are different from the other curves.
- For a specific upstream depth, h_u, an increase in discharge corresponds to a decrease in submergence. This is because $S= h_d/h_u$; if the flow rate increases, the downstream depth decreases, consequently reducing the submergence.

Calibrations of Non-Orifice Discharge Equations for Free- and Submerged-Flow Conditions

Based on Eqs. 1 and 2 presented in Chapter II for free and submerged non-orifice flow, calibration of the laboratory data was accomplished. Tables 3 and 4 present the coefficient values for free and submerged flow, respectively. To measure the accuracy of the predictions, the coefficient of determination, r^2, and the standard error of the estimate, SEE, were used, where SEE was defined as follows:

$$SEE = \sqrt{\frac{\sum (y - y')^2}{n}} \tag{11}$$

where y are the measured values; y' are the estimated values; and n is the number of values. Figure 17 and 18 shows the high correlation between the discharges obtained using the traditional equation (Eqs. 1 and 2), and discharges measured in the laboratory.

Table 3. Free Non-Orifice Calibration

	Parameter			
Condition	C_f	n_{f1}	r^2	SEE (m^3/s)
Free Flow	0.989	1.493	0.995	2.34E-03

The free-flow equation (see Table 3) is:

$$Q_f = 0.99(h_u)^{1.49} \qquad (12)$$

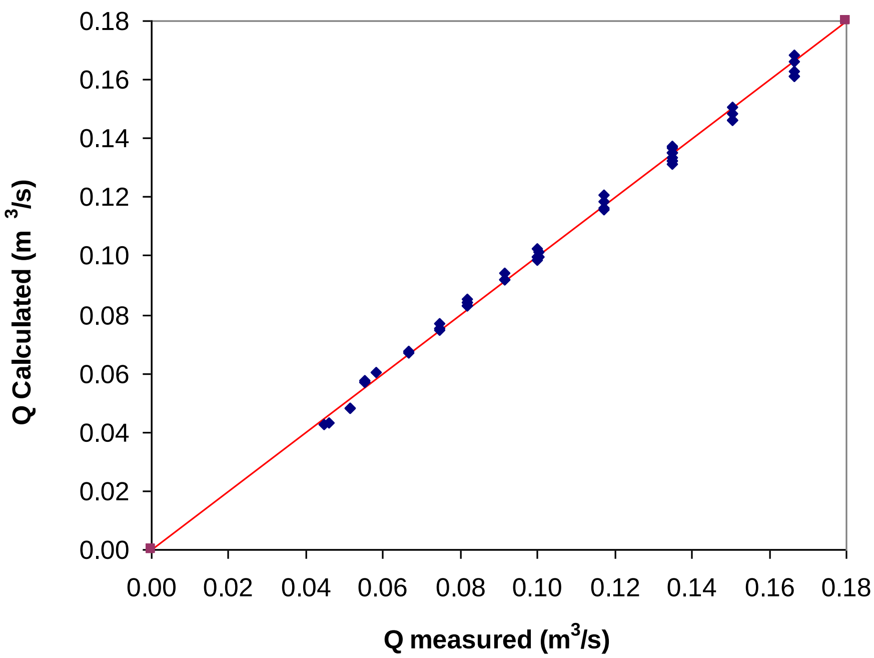

Fig.17. Measured and calculated flow rates for a free non-orifice regime

Table 4. Submerged Flow Non-orifice Calibration

	Parameter				
Condition	C_s	n_{f2}	n_s	r^2	SEE (m^3/s)
Submerged Flow	0.704	1.426	-0.976	0.981	3.30E-03

The submerged-flow equation is (see Table 4):

$$Q_s = \frac{0.704\,(h_u - h_d)^{1.426}}{-\log(S)^{0.976}} \tag{13}$$

where Q_f is the discharge (m^3/s); C_f is the free-flow coefficient; n_f is the free-flow exponent; C_s is the submerged-flow coefficient; n_s is the submerged–flow exponent; and S is the submergence.

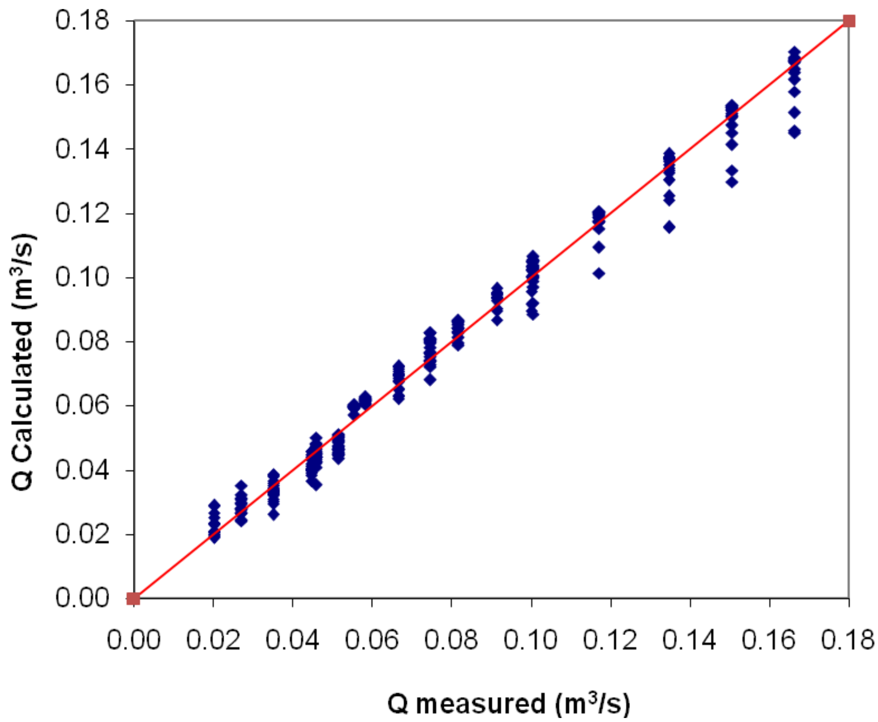

Fig.18. Measured and calculated flow rates calibration for a submerged non-orifice regime

Transition Between Non-orifice and Orifice Regimes

The transition regime is defined as the condition where the flow passes from non-orifice to orifice, or vice versa, and a range is defined by this regime. The depth upstream at the gate is not uniform, due to the contraction at the section of the gate. The distribution of vertical upstream depth is not equal that lateral depth and it generate a range in the transition, which was defined by two thresholds: non-orifice transition threshold, h_{NOt} and orifice transition threshold, h_{Ot}.

The non-orifice transition threshold, h_{NOt}, is the initial condition of the transition, when water upstream reaches the gate lip. Figure 19a shows an example of this hydraulic condition. The threshold determines when the gate affects the flow,and h_{NOt} is compared with other depths to define the non-orifice flow condition. Equation 14 is the condition for a non-orifice regime:

$$h_u < h_{NO_t} \tag{14}$$

The orifice transition threshold, h_{Ot}, is when the gate operates under orifice conditions (Fig. 19b). It means that the upstream water level at the gate has complete hydraulic seal. It is defined as a depth to define the orifice-flow condition. Equation 15 is the condition for an orifice regime:

$$h_u > h_{O_t} \tag{15}$$

The range of transition from non-orifice to orifice regimes depends on the average velocity of the flow at the gate, and also on the submergence. When there are lower velocities or high submergence, there is a narrower transition range. Sometimes, the difference between these two situations is minimal. Therefore, it is possible to have only one transition point (not a range), especially for high submergence values. When there are high velocities at the gate or lower submergence, there is a relatively large transition range. The definition of this range will be presented in the following section of this chapter.

Figure 19 shows two kinds of conditions: (1) For the non-orifice transition threshold, the water initially touches the face of the gate near the center of the channel, making a semicircle, note that the flow in the corners do not touch by the gate; and, (2) the upstream depth increases in the center and in the corners until the orifice transition threshold is reached, in which there is sufficient hydraulic seal to cause orifice flow conditions.

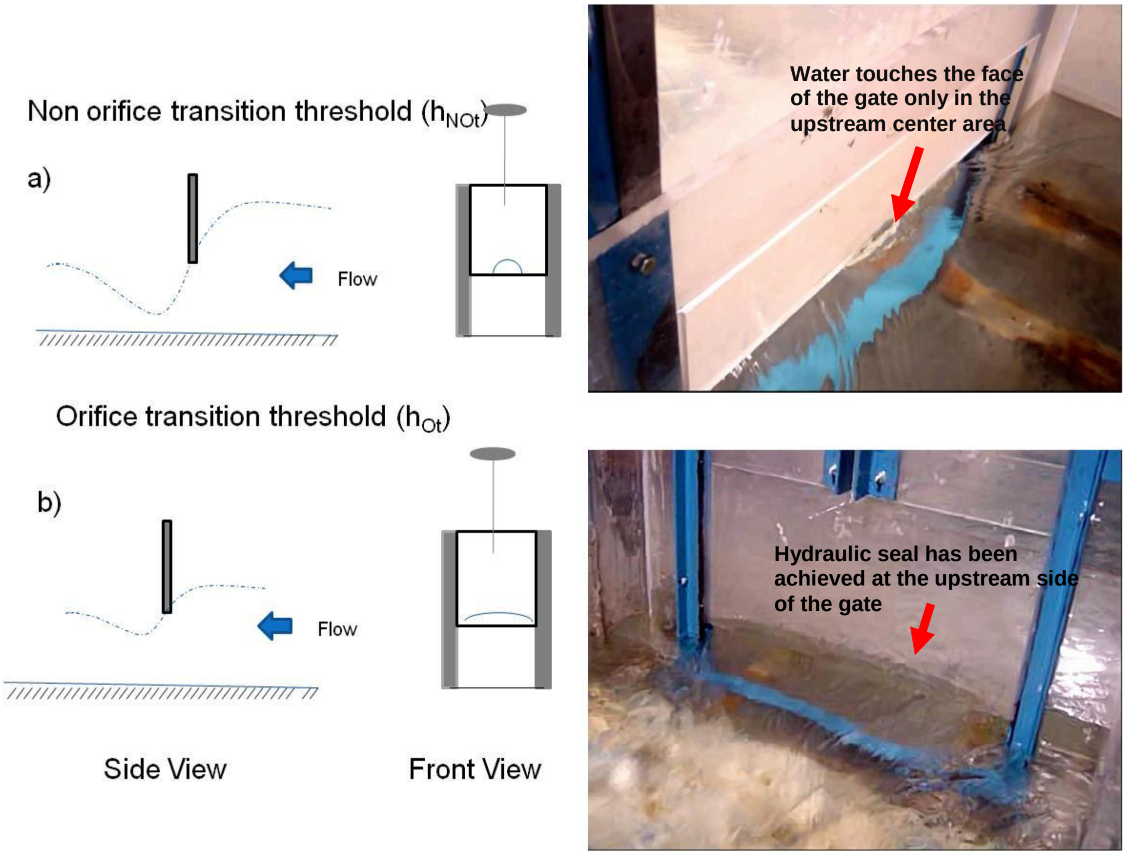

Fig. 19. Flow characteristics in the transition zone: (a) non-orifice transition threshold; and (b) orifice transition threshold

Defining the Flow Regime Transition:
Non-Orifice-to-Orifice

Three different approaches were used to estimate the flow-regime transition limits. Each of these is described in the following subsections.

First Approach: Using an Empirical Equation
to Describe the Threshold

The first approach was to find equations that describe the laboratory data, in the transition zone, searching the relationship among discharge, upstream depth, submergence, and gate opening. All of the equation forms included in this study describe the laboratory data very well. Table 5 shows equations that were developed for this purpose with the respective coefficient of determination, r^2, and SEE.

Table 5. Equations Used to Model the Laboratory Data

No.	Equation	r^2	SEE (m)	a	b	c
I	$h_{NO_t} = aQ + bG_o + c$	0.998	0.0032	0.202	0.932	0.013
II	$h_{NO_t} = aQ^2 + bQ + aG_o^2 + bG_o$	0.996	0.0064	1.025	-0.030	-
III	$h_{NO_t} = aS + bG_o + c$	0.996	0.0043	-0.056	1.011	0.057
IV	$h_{NO_t} = aQ^2 + G_o$	0.996	0.0068	1.111	-	-

In each of the equations presented in Table 5, Q is the flow rate (m^3/s); G_o is the gate opening (m); h_{NOt} is the upstream non-orifice transition threshold depth (m); and the letters a, b, c are the fitted equation parameters.

In Fig. 20, bars represent the standard error of the estimate, and the line represents the value of r^2. The results of this analysis show that equation that best fits the laboratory data is Eq. I, with a coefficient of determination equal to 0.998, and SEE of 3.2 mm. Even though there are equations that describe the data very well, the critical issue with this approach is that these are empirical equations and their use requires site-specific calibration of the three parameters (a, b, and c). Thus, care must be exercised in the use of these equations.

Second Approach: Using the Traditional Submerged Non-orifice Equation to Describe the Regime Threshold

Equation 2 is the traditional formula that was used to calculate the discharge. The results were compared with the measured discharge in the laboratory, calculating the percent error, which was plotted versus the number of measured data points. The valued of C_f, n_f and n_s from

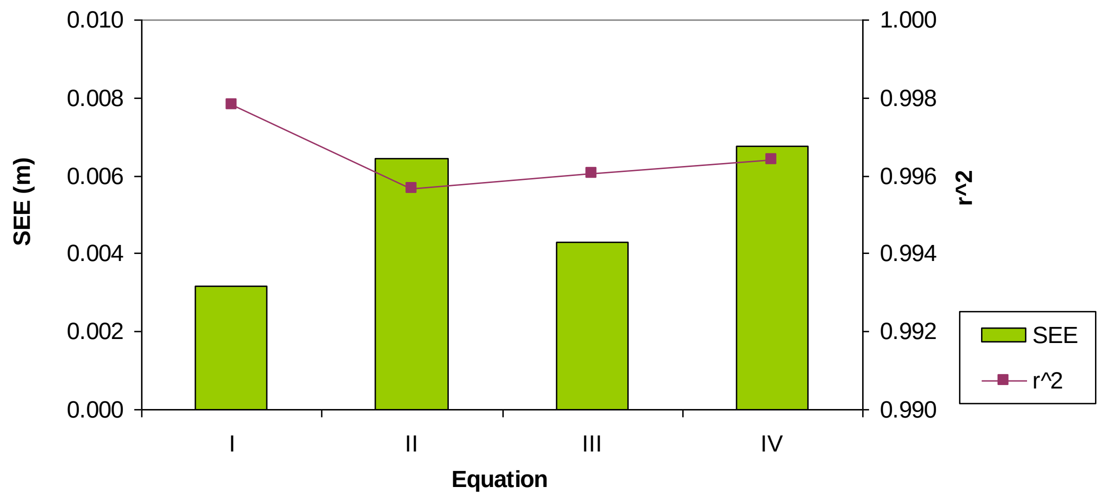

Fig. 20. Coefficient of determination, r^2, and standard error of the estimate, SEE, for the proposed equations, as compared to the laboratory water depth data

Eq. 2 were determined by taking the data for submerged flow conditions for different flow rates. Figure 21 and Table 6 show an example of this calculation for a discharge of 0.117 m^3/s and a G_o of 0.30 m. It was found that the percent error, using the submerged non-orifice equation, suddenly changed at point 14 where the absolute value of the percent error began to increase. This point coincided with the observed non-orifice to orifice transition threshold in the laboratory.

Table 6 shows the comparison between measured and calculated discharge using the traditional submerged non-orifice equation (Eq. 2). Columns 1 to 3 correspond to measured data collected in the laboratory, for a constant discharge, where the tail gate was raised to a different angle, causing the flow regime to change from non-orifice to orifice (see experimental procedure, Chapter III). The fifth column shows the percent discharge error, and the change from positive to negative at point 14, where the absolute value of the error begins to increase.

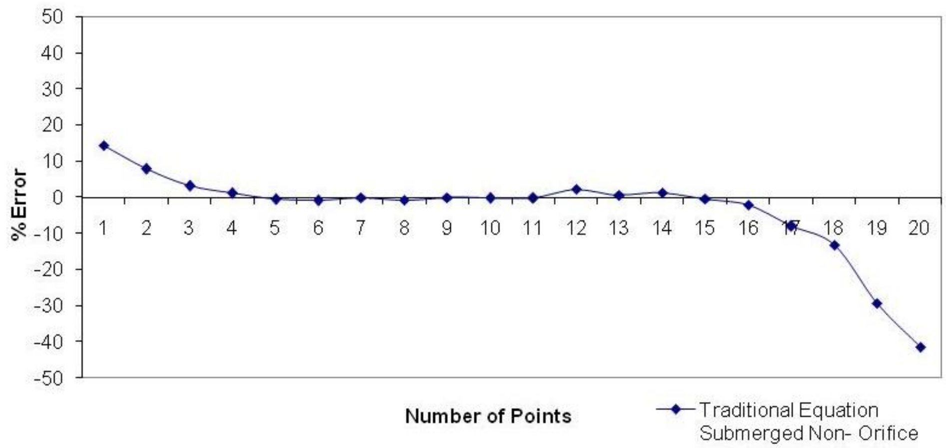

Fig. 21. Difference in error between calculated and measured discharge versus number of points measured for a discharge of 0.117 m^3/s and G_o of 0.30 m

Table 6. Measured and Estimated Discharge for 0.117 m^3/s and a G_o of 0.30 m

	Laboratory		Traditional Equation Submerged Non- Orifice (Eq. 2)	
Trial	Gate Status	Q (m^3/s)	Q estimated (m^3/s)	% Error
1	Non Orifice	0.117	0.100	14
2	Non Orifice	0.117	0.108	8
3	Non Orifice	0.117	0.114	3
4	Non Orifice	0.117	0.116	1
5	Non Orifice	0.117	0.118	-1
6	Non Orifice	0.117	0.118	-1
7	Non Orifice	0.117	0.117	0
8	Non Orifice	0.117	0.118	-1
9	Non Orifice	0.117	0.117	0
10	Non Orifice	0.117	0.117	0
11	Non Orifice	0.117	0.117	0
12	Non Orifice	0.117	0.115	2
13	Transition Non-Orifice & Orifice	0.117	0.116	1
14	Transition Non-Orifice & Orifice	0.117	0.116	1
15	Orifice	0.117	0.118	-1
16	Orifice	0.117	0.120	-2
17	Orifice	0.117	0.127	-8
18	Orifice	0.117	0.133	-13
19	Orifice	0.117	0.151	-29
20	Orifice	0.117	0.166	-42

Most of the data show one point where there was a sudden change from positive to negative, and then an increase in error. However, in some cases, these points do not coincide with the laboratory observations, especially for lower discharges (less than 0.1 m^3/s). Appendix V shows the curves for other measured discharges through the sluice gate.

Third Approach: Using the Specific Energy Equation to Describe the Regime Threshold

The third approach to define the regime transition was using the specific-energy equation, which was compared with experimental observations. The transition range is defined by two conditions: non-orifice transition threshold, and orifice transition threshold.

Estimation of Non-Orifice Transition Threshold, h_{Not}, Using the Specific-Energy Equation

This first condition is when the upstream water surface touches the lip of the gate and the flow is affected by the gate opening; in such cases, the flow regime can be estimated using the specific-energy equation (Jeppson 2001). Figure 22 shows the location of measured water depths at sections 1 and 2.

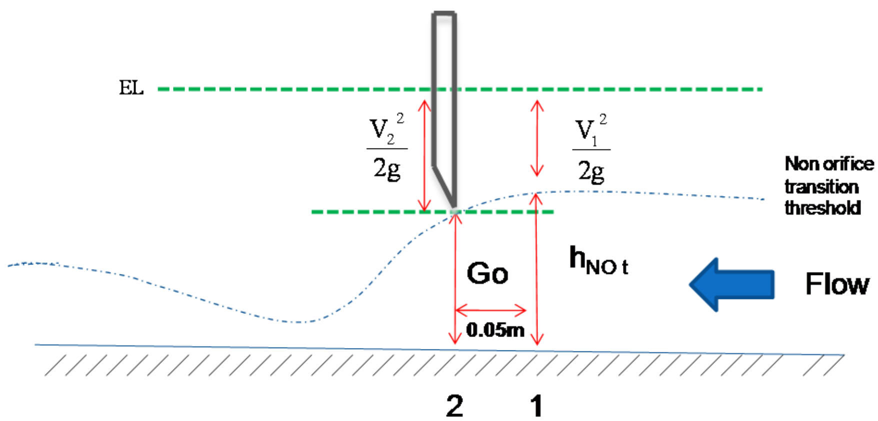

Fig. 22. Channel side view, showing the non-orifice transition threshold (EL is the energy line)

At the upstream location (section 1), the specific energy is equal to the non-orifice transition threshold (h_{NOt}) plus the velocity head. In section 2 (directly under the gate), the energy is equal to the water depth at the gate structure (the gate opening, G_o), plus the velocity head at the same location. In the laboratory it was observed that, in section 2, water flows under the gate, and vertical and horizontal contraction occurs, causing the average velocity at the gate to increase and the depth to decrease. Thus, when the velocity head ($V^2/2g$) under the gate increases, the water depth at the gate structure must decrease proportionately. Using these criteria, the upstream depth at section 2 was calculated.

Applying the specific-energy equation between sections 1 and 2, and neglecting friction losses:

$$E_1 = E_2 \tag{16}$$

$$G_o + \frac{V_2^2}{2g} = h_{NOt} + \frac{V_1^2}{2g} \tag{17}$$

$$h_{NOt} = G_o + \frac{V_2^2}{2g} - \frac{V_1^2}{2g} \tag{18}$$

$$h_{NOt} = G_O + \frac{Q^2}{2g}\left(\frac{1}{A_2^2} - \frac{1}{A_1^2}\right) \tag{19}$$

The correlation for non-orifice transition threshold between measured and estimated upstream water depth values using Eq. 19 is presented in Fig. 23.

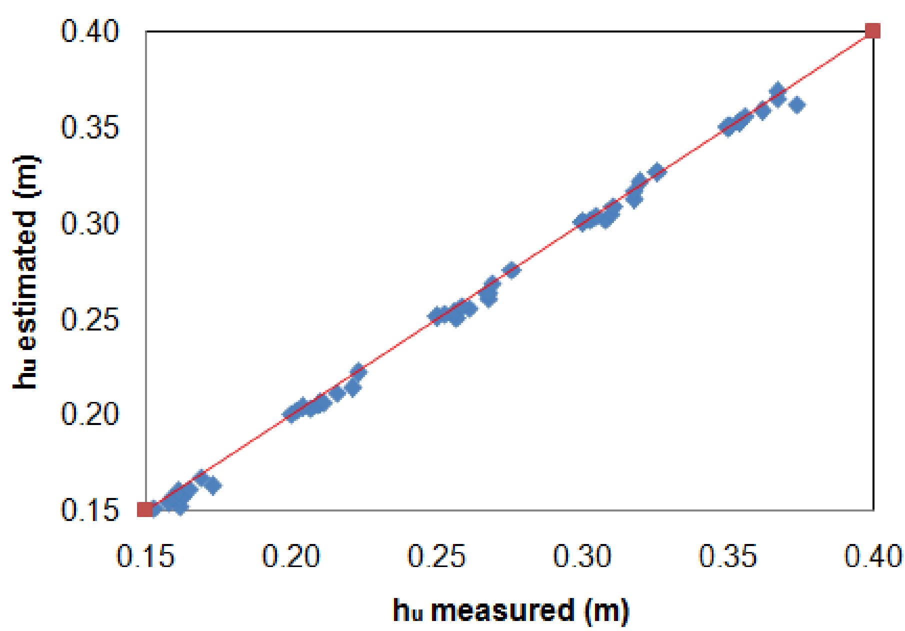

Fig. 23. Measured and estimated upstream depths at the non-orifice transition threshold

Estimation of Orifice Transition Threshold, h_{Ot}, Using the Specific-Energy Equation

This second condition is when gate operates under an orifice flow regime (where upstream hydraulic seal is achieved). The procedure to estimate the upstream depth for this condition is the same as that calculated for the non-orifice transition threshold, using the specific-energy equation, with the assumption that the water level at the gate is equal to h_{NOt} (see Fig. 24).

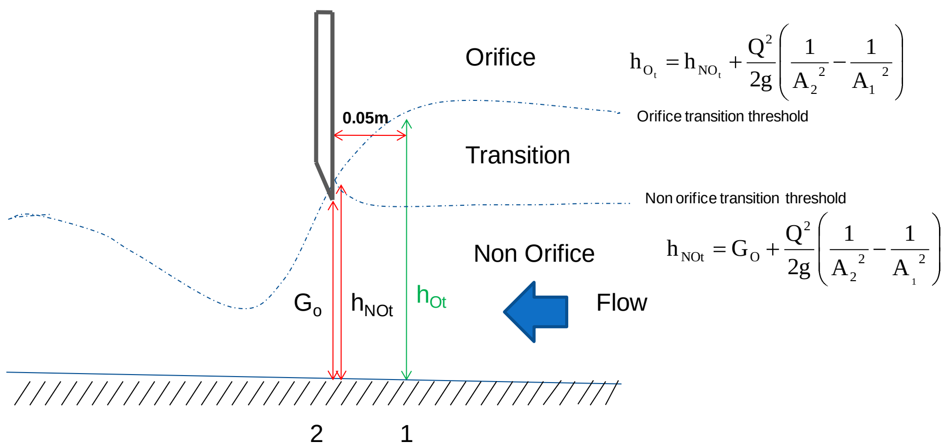

Fig. 24. Flow characteristics for non-orifice and orifice transition thresholds

Calculating the orifice transition threshold, h_{Ot}, using the specific-energy equation between sections 1 and 2:

$$h_{NO_t} + \frac{V_2{}^2}{2g} = h_{O_t} + \frac{V_1{}^2}{2g} \tag{20}$$

where the bottom edge of the sluice gate is touched by the surface of the water. Assuming that the depth in section 2 is the same as h_{Not}:

$$h_{O_t} = h_{NO_t} + \frac{V_2{}^2}{2g} - \frac{V_1{}^2}{2g} \tag{21}$$

$$h_{O_t} = h_{NO_t} + \frac{Q^2}{2g}\left(\frac{1}{A_2^{\,2}} - \frac{1}{A_1^{\,2}}\right) \tag{22}$$

where h_{NOt} is the upstream depth, which defines the non-orifice transition threshold; h_{Ot} is the upstream depth, which defines the orifice transition threshold; and, $V^2/2g$ is the velocity head.

The correlation for orifice transition threshold between measured and estimated upstream water depth values using Eq. 22 are presented in Fig. 25.

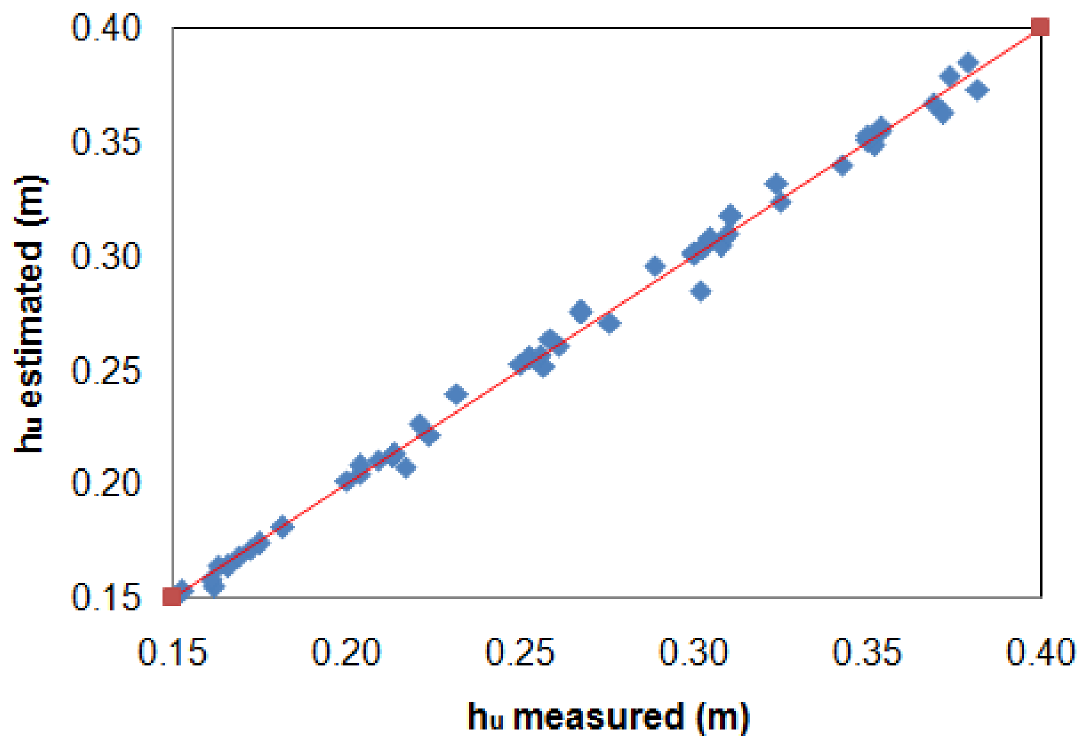

Fig. 25. Measured and estimated upstream depths at the orifice transition threshold

An application of Eqs. 19 and 22 and their effect on the submergence is shown in Fig. 26 for a gate opening of 0.30 m, it is noted that the transition range between non-orifice and orifice regimes has a relationship with the submergence. At high submergence, the range is shorter, and vice versa. Figure 27 shows the effect of the submergence for gate opening of 0.15, 0.20, 0.25, 0.30 and 0.35 m.

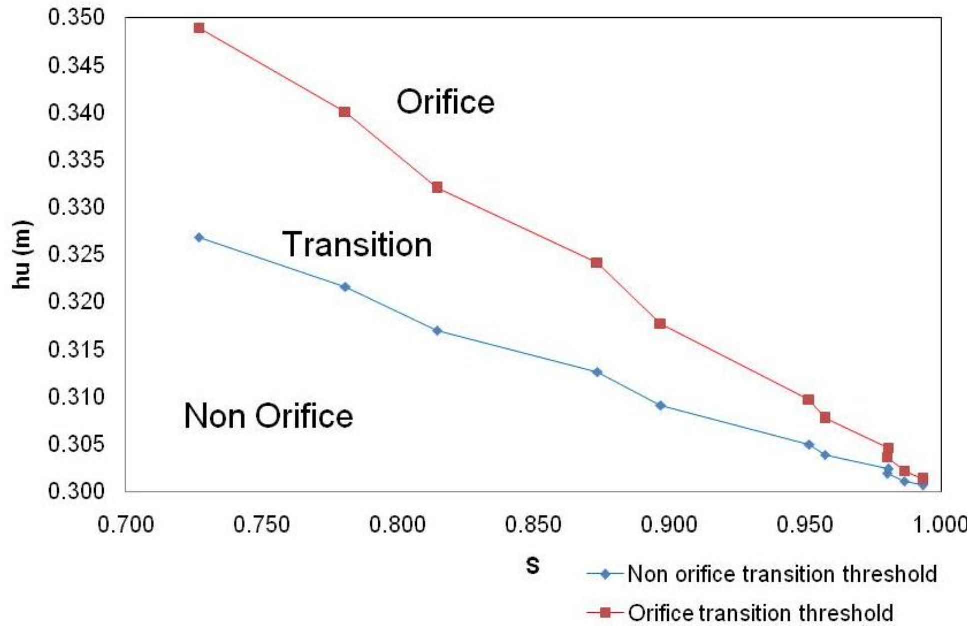

Fig. 26. Upstream depth and submergence distinguishing non-orifice, transition, and orifice regimes for G_o = 0.3 m

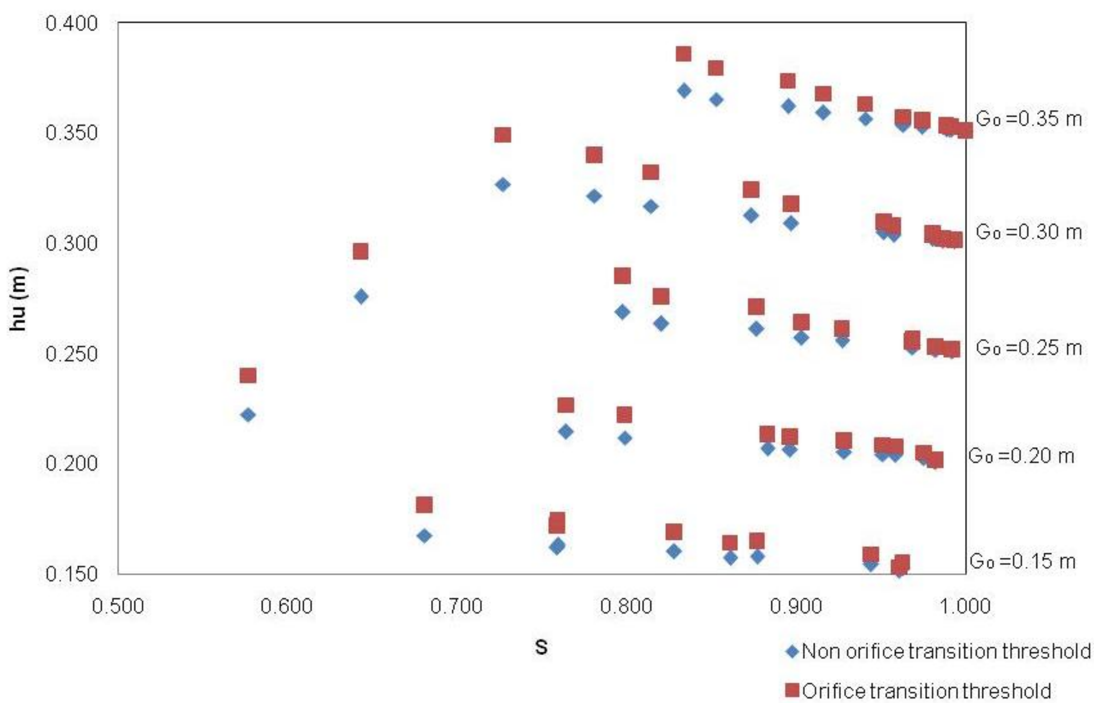

Fig. 27. Submergence vs. upstream depth to gate openings of 0.15, 0.20, 0.25, 0.3, and 0.35 m

Note that with high submergence, the range of transition is shorter, and vice versa (Fig. 27).

In conclusion, using simple equations based on the specific-energy equation it is possible to know the boundaries between non-orifice and orifice flow regimes. Equations 14 and 19 can be used to define the limit of the non-orifice condition, while Eqs. 15 and 22 can be used to define the limit of the orifice condition. Appendix VI shows application to determine, non-orifice and orifice transition threshold, using specific energy equation.

Estimation of the Transition Coefficient (C_o)

The transition coefficient is a dimensionless parameter that measures the ratio of gate opening and upstream water depth. It was used to determine whether the gate is operating under orifice or non-orifice conditions. And, it could be applied in a hydraulic simulation because such a model must allow the possibility that flow might change from a regime to another. C_o can be expressed as:

$$C_o = \frac{G_o}{h_u} \tag{23}$$

where C_o is the transition coefficient. The identification of C_o has been considered in previous research. Garbrecht (1977) collected many data points at canal gate structures in the field and reported that there was a condition when the orifice flow became almost non-orifice flow. He found that the ratio of the gate opening to the upstream water depth ($C_o = G_o/h_u$) is 0.83. Nguyen (2000) called this condition as constriction coefficient and reported that $0.90 \leq C_o \leq 0.98$ for a rectangular gate of b = 0.29 m and G_w = 0.22 m. However, there is no published research that defines the transition.

As a presented in the previous section, the non-orifice to orifice regime transition is defined by two conditions (Eqs. 19 and 22). Consequently, the transition coefficient ($C_o = G_o/h_u$) should be defined as:

$$C_{o(No_t)} = \frac{G_o}{h_{No_t}} \tag{24}$$

and

$$C_{O(O_t)} = \frac{G_o}{h_{O_t}} \tag{25}$$

where $C_{o(Not)}$ is the coefficient of non-orifice transition threshold; $C_{o(Ot)}$ is the coefficient of orifice transition threshold; h_{Not} is the upstream depth to define the non-orifice threshold; and, h_{Ot} is the upstream depth to define the orifice threshold.

The range of the C_o value to define the transition between non-orifice and orifice regimes was analyzed. Data collected in the laboratory were used to determine the range of C_o. Table 7 shows the laboratory data and calculated values.

The results indicate that data in the non-orifice condition, and in the transition zone, has good behavior (less error between measured and estimated C_o). Figure 28 shows that the majority of the data points are within ±5% error.

C_o is not a unique value. The experimental result shows that the range of transition coefficient between 0.83 and 1.00 has a relationship with the submergence. Equations 26 and 27 determine the curves of interpolation of the points in non-orifice; orifice transition threshold and the submergence.

$$C_{o_{(NO_t)}} = -1.114S^3 + 2.95S^2 - 2.2881S + 1.450 \tag{26}$$

$$C_{o_{(O_t)}} = -1.124S^3 + 3.330S^2 - 2.717S + 1.506 \tag{27}$$

Figure 29 shows the effects on the submergence in the transition coefficient, for lower submergence values, there are major ranges in the transition coefficient. For example, the range of C_o between 0.83 and 0.90 correspond to a submergence of 0.57, while a range of C_o between 0.998 and 0.999 corresponds to submergence near unity.

Table 7. Measured and Calculated Upstream Depth values, and Calculated C_o, for h_{NOt} and h_{Ot}, for Different Discharges and Gate Openings

			Measured				Estimated			
			Depth Upstream Threshold (m)		Co		Depth Upstream Threshold (m)		Co	
Go	Q (m3/s)	S	Non orifice transition threshold	Orifice transition threshold	Non orifice transition threshold	Orifice transition threshold	Non orifice transition threshold	Orifice transition threshold	Non orifice transition threshold	Orifice transition threshold
0.15	0.020	0.961	0.153	0.153	0.98	0.98	0.151	0.153	0.99	0.98
	0.027	0.963	0.162	0.162	0.93	0.93	0.153	0.155	0.98	0.97
	0.035	0.944	0.158	0.161	0.95	0.93	0.154	0.159	0.97	0.95
	0.045	0.861	0.159	0.166	0.95	0.91	0.157	0.164	0.95	0.91
	0.046	0.877	0.163	0.163	0.92	0.92	0.158	0.165	0.95	0.91
	0.051	0.828	0.161	0.169	0.93	0.89	0.160	0.169	0.94	0.89
	0.055	0.759	0.165	0.172	0.91	0.87	0.162	0.172	0.93	0.87
	0.058	0.759	0.173	0.175	0.87	0.86	0.163	0.174	0.92	0.86
	0.066	0.681	0.169	0.182	0.89	0.83	0.168	0.181	0.90	0.83
0.20	0.020	0.982	0.200	0.200	1.00	1.00	0.201	0.202	1.00	0.99
	0.035	0.975	0.202	0.204	0.99	0.98	0.202	0.205	0.99	0.98
	0.045	0.958	0.207	0.217	0.97	0.92	0.204	0.208	0.98	0.96
	0.046	0.951	0.204	0.204	0.98	0.98	0.204	0.208	0.98	0.96
	0.051	0.928	0.209	0.209	0.96	0.96	0.205	0.210	0.97	0.95
	0.055	0.897	0.210	0.213	0.95	0.94	0.206	0.212	0.97	0.94
	0.058	0.883	0.211	0.214	0.95	0.94	0.207	0.213	0.97	0.94
	0.075	0.799	0.216	0.224	0.93	0.89	0.212	0.222	0.94	0.90
	0.082	0.764	0.221	0.221	0.91	0.91	0.214	0.226	0.93	0.88
	0.100	0.577	0.223	0.232	0.90	0.86	0.222	0.240	0.90	0.83
0.25	0.027	0.992	0.257	0.257	0.97	0.97	0.251	0.252	1.00	0.99
	0.035	0.982	0.250	0.250	1.00	1.00	0.252	0.253	0.99	0.99
	0.046	0.968	0.253	0.253	0.99	0.99	0.253	0.255	0.99	0.98
	0.051	0.969	0.256	0.256	0.98	0.98	0.253	0.257	0.99	0.97
	0.066	0.927	0.261	0.261	0.96	0.96	0.256	0.261	0.98	0.96
	0.075	0.903	0.259	0.259	0.97	0.97	0.257	0.264	0.97	0.95
	0.091	0.877	0.268	0.276	0.93	0.91	0.261	0.271	0.96	0.92
	0.100	0.820	0.267	0.267	0.94	0.94	0.263	0.275	0.95	0.91
	0.100	0.821	0.268	0.268	0.93	0.93	0.264	0.276	0.95	0.91
	0.117	0.798	0.269	0.302	0.93	0.83	0.269	0.285	0.93	0.88
	0.135	0.643	0.276	0.289	0.91	0.87	0.276	0.296	0.91	0.84
0.30	0.027	0.993	0.300	0.300	1.00	1.00	0.301	0.301	1.00	1.00
	0.035	0.987	0.300	0.300	1.00	1.00	0.301	0.302	1.00	0.99
	0.046	0.980	0.303	0.303	0.99	0.99	0.302	0.304	0.99	0.99
	0.051	0.980	0.308	0.308	0.98	0.98	0.302	0.305	0.99	0.98
	0.066	0.957	0.305	0.305	0.98	0.98	0.304	0.308	0.99	0.97
	0.075	0.952	0.310	0.310	0.97	0.97	0.305	0.310	0.98	0.97
	0.100	0.897	0.311	0.311	0.97	0.97	0.309	0.318	0.97	0.94
	0.117	0.874	0.318	0.325	0.94	0.92	0.313	0.324	0.96	0.93
	0.135	0.815	0.318	0.324	0.94	0.93	0.317	0.332	0.95	0.90
	0.151	0.781	0.320	0.343	0.94	0.88	0.322	0.340	0.93	0.88
	0.166	0.727	0.326	0.352	0.92	0.85	0.327	0.349	0.92	0.86
0.35	0.027	1.000	0.350	0.350	1.00	1.00	0.350	0.351	1.00	1.00
	0.046	0.991	0.351	0.351	1.00	1.00	0.351	0.353	1.00	0.99
	0.051	0.989	0.350	0.350	1.00	1.00	0.352	0.353	1.00	0.99
	0.066	0.975	0.354	0.354	0.99	0.99	0.353	0.356	0.99	0.98
	0.075	0.963	0.354	0.354	0.99	0.99	0.354	0.357	0.99	0.98
	0.100	0.941	0.356	0.372	0.98	0.94	0.357	0.363	0.98	0.96
	0.117	0.916	0.362	0.369	0.97	0.95	0.359	0.368	0.97	0.95
	0.135	0.895	0.374	0.382	0.94	0.92	0.362	0.373	0.97	0.94
	0.151	0.853	0.367	0.374	0.95	0.94	0.365	0.379	0.96	0.92
	0.166	0.834	0.367	0.379	0.95	0.92	0.369	0.386	0.95	0.91

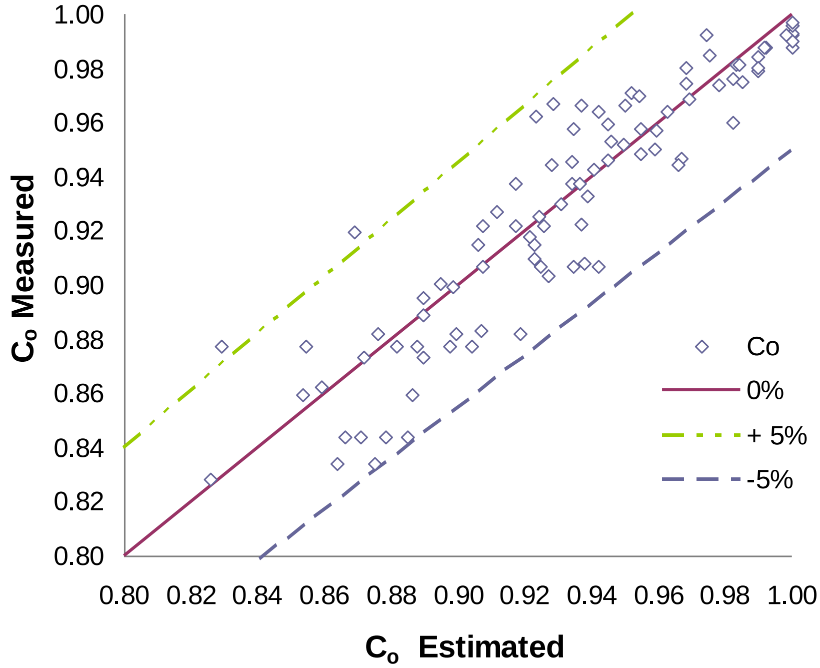

Fig. 28. Measured versus estimated transition coefficient, C_o

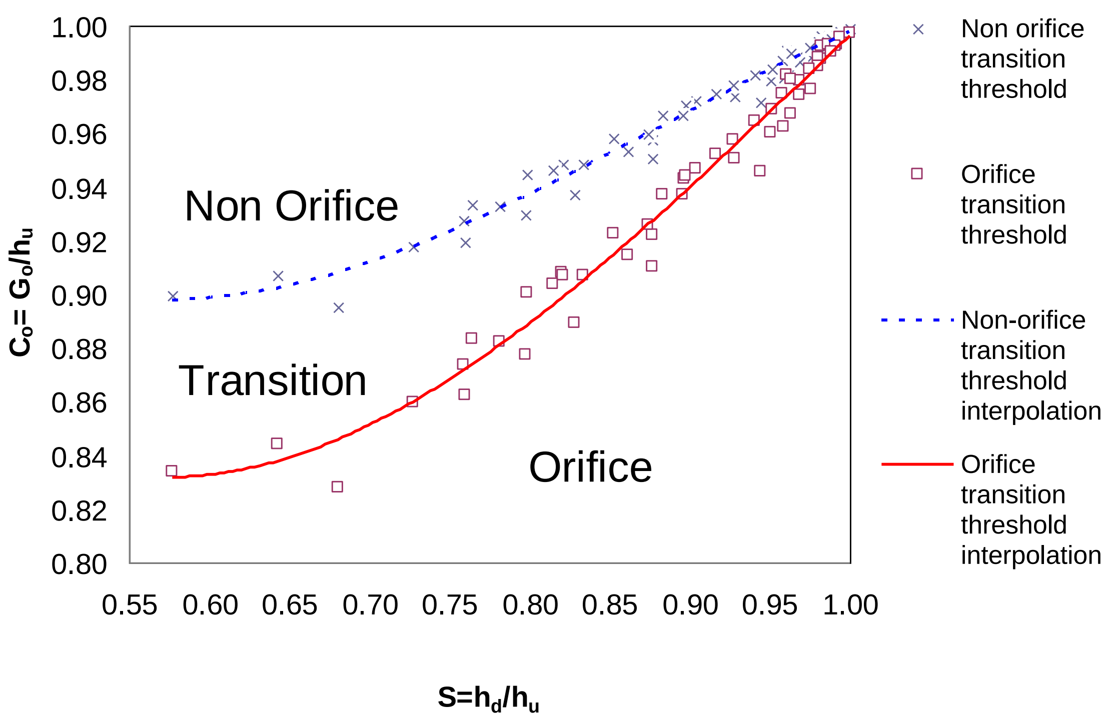

Fig. 29. Effect of submergence on the estimated value of C_o

Figure 29 can be used as a simple guide for identifying the flow regime condition in gate. Given h_u, h_d, G_o, it is possible to determine if it is non-orifice, transition or orifice. For example, Table 8 shows three cases, which were collected data in the laboratory. It is noted that in all cases, C_o varies from 0.83 to 1.00, and G_o is equal to 0.30 m, to allow fair comparisons.

For cases one and two, would be possible to obtain the same C_o and different flow condition because the submergence values are different. Cases one and three both have the same flow rate and gate opening, but the flow conditions (regimes) are different. The flow regime found using Fig. 29 coincides with the observation in the laboratory. Thus, Fig. 29 can be useful to determine the flow condition.

Table 8. Sample Applications to Determine Flow Regime Using Fig. 29

Cases	Q (m^3/s)	G_o (m)	h_u (m)	h_d (m)	C_o	S	Flow Condition using Fig. 29.
1	0.166	0.3	0.32	0.19	0.94	0.59	Non-orifice
2	0.066	0.3	0.32	0.31	0.94	0.97	Orifice
3	0.166	0.3	0.34	0.23	0.88	0.68	Transition

When the transition coefficient, C_o, is greater than 1.00, it always corresponds to a non-orifice flow condition, and a C_o lower than 0.83 always indicates an orifice flow regime. The definition of the regime when C_o is between 0.83 and 1.0 requires consideration of the submergence; in such cases, Fig. 29 is used to determine the flow condition.

Application of Fig. 29 to Determine the Correct Discharge Equation

Identification of the flow regime is necessary to determine the correct equation to apply. Thus, Fig. 29 can be used to determine the different flow conditions (non-orifice, transition and orifice). Table 9 shows h_u and h_d values (column 2 and 3) for a rectangular gate structure under different discharges and flow conditions. To determine the flow condition and discharge, it is necessary to calculate values of C_o (G_o/h_u) and S (h_d/h_u). Then, using Fig. 29, the different flow conditions: non-orifice, transition and orifice are determined. Also, the flow rate is estimated using the traditional equations: submerged non orifice (Eq. 2) and submerged orifice (Eq. 4). It was noted that using the submerged non-orifice equation (Eq. 2) provided good results in the computation of the discharge of the transition regime between non-orifice and orifice flow regimes. In general, comparisons between discharges measured and estimated in Table 9 show a good fit, according to the low percentage of error.

Development of a Unique Equation for Non-Orifice Flow Conditions

In this section, it is shown the results regarding whether a single equation can be used to describe free and submerged non-orifice flow through the gate. Laboratory data for a non-orifice flow regime was used; some of these data are shown in Fig. 30, which is a plot of two variables: submergence and upstream depth. Since the non-orifice flow condition is independent of the gate opening, the highest G_o (0.35 m) was chosen.

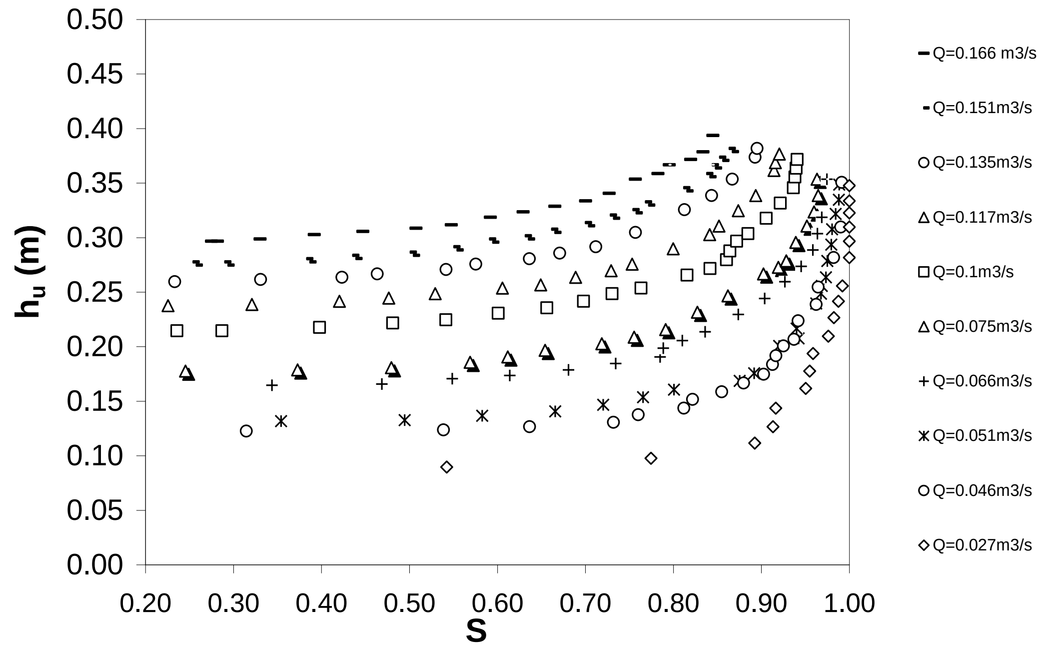

Fig. 30. Upstream water depth (h_u) versus submergence (S) (G_o = 0.35 m) for a non-orifice flow regime

Table 9. Sample Applications to Determine the Correct Equation to Apply

Measured			Estimated				
Q (m^3/s)	h_u (m)	h_d (m)	C_o	S	Flow Condition using Fig. 29	Q (m^3/s)	%Error
0.117	0.249	0.132	1.41	0.53	Non-Orifice	0.118	-0.7
0.117	0.254	0.154	1.38	0.61	Non-Orifice	0.118	-1.1
0.117	0.257	0.167	1.36	0.65	Non-Orifice	0.117	-0.3
0.117	0.264	0.182	1.33	0.69	Non-Orifice	0.118	-1.2
0.117	0.270	0.197	1.30	0.73	Non-Orifice	0.118	-0.4
0.117	0.276	0.208	1.27	0.75	Non-Orifice	0.118	-0.7
0.117	0.290	0.232	1.21	0.80	Non-Orifice	0.118	-0.7
0.117	0.303	0.255	1.16	0.84	Non-Orifice	0.115	1.7
0.117	0.311	0.265	1.13	0.85	Non-Orifice	0.116	0.6
0.117	0.325	0.284	1.08	0.87	Non-Orifice	0.116	0.6
0.117	0.339	0.303	1.03	0.89	Non-Orifice	0.115	1.6
0.117	0.362	0.331	0.97	0.91	Transition Non-Orifice & Orifice	0.116	1.2
0.117	0.369	0.338	0.95	0.92	Transition Non-Orifice & Orifice	0.118	-0.8
0.117	0.377	0.347	0.93	0.92	Orifice	0.113	3.3
0.117	0.393	0.363	0.89	0.92	Orifice	0.113	3.3
0.117	0.423	0.390	0.83	0.92	Orifice	0.119	-1.5
0.135	0.271	0.147	1.29	0.54	Non-Orifice	0.133	1.1
0.135	0.276	0.159	1.27	0.58	Non-Orifice	0.136	-0.6
0.135	0.281	0.179	1.25	0.64	Non-Orifice	0.135	-0.3
0.135	0.286	0.192	1.23	0.67	Non-Orifice	0.135	-0.5
0.135	0.292	0.208	1.20	0.71	Non-Orifice	0.135	0.1
0.135	0.305	0.231	1.15	0.76	Non-Orifice	0.136	-0.9
0.135	0.326	0.265	1.07	0.81	Non-Orifice	0.137	-1.5
0.135	0.339	0.286	1.03	0.84	Non-Orifice	0.135	-0.4
0.135	0.354	0.307	0.99	0.87	Non-Orifice	0.135	-0.2
0.135	0.374	0.334	0.94	0.89	Transition Non-Orifice & Orifice	0.134	0.8
0.135	0.382	0.342	0.92	0.90	Orifice	0.131	2.9
0.135	0.390	0.351	0.90	0.90	Orifice	0.129	4.1
0.135	0.408	0.366	0.86	0.90	Orifice	0.134	0.5
0.135	0.439	0.396	0.80	0.90	Orifice	0.136	-0.7
0.151	0.287	0.144	1.22	0.50	Non-Orifice	0.146	3.0
0.151	0.292	0.161	1.20	0.55	Non-Orifice	0.148	1.4
0.151	0.299	0.177	1.17	0.59	Non-Orifice	0.152	-0.7
0.151	0.302	0.191	1.16	0.63	Non-Orifice	0.151	-0.1
0.151	0.308	0.204	1.14	0.66	Non-Orifice	0.152	-1.0
0.151	0.314	0.220	1.12	0.70	Non-Orifice	0.152	-0.6
0.151	0.321	0.234	1.09	0.73	Non-Orifice	0.152	-0.9
0.151	0.326	0.246	1.07	0.75	Non-Orifice	0.151	0.0
0.151	0.333	0.256	1.05	0.77	Non-Orifice	0.152	-1.2
0.151	0.346	0.281	1.01	0.81	Non-Orifice	0.150	0.7
0.151	0.359	0.301	0.98	0.84	Non-Orifice	0.149	1.0
0.151	0.367	0.310	0.95	0.84	Non-Orifice	0.152	-0.7
0.151	0.374	0.319	0.94	0.85	Transition Non-Orifice & Orifice	0.153	-1.3
0.151	0.382	0.330	0.92	0.86	Orifice	0.149	0.9
0.151	0.414	0.364	0.85	0.88	Orifice	0.146	2.9
0.151	0.448	0.394	0.78	0.88	Orifice	0.152	-1.0
0.166	0.309	0.157	1.13	0.51	Non-Orifice	0.163	2.2
0.166	0.312	0.171	1.12	0.55	Non-Orifice	0.164	1.5
0.166	0.319	0.189	1.10	0.59	Non-Orifice	0.167	-0.2
0.166	0.324	0.204	1.08	0.63	Non-Orifice	0.167	-0.7
0.166	0.329	0.219	1.07	0.67	Non-Orifice	0.167	-0.5
0.166	0.334	0.234	1.05	0.70	Non-Orifice	0.166	0.2
0.166	0.341	0.248	1.03	0.73	Non-Orifice	0.166	-0.1
0.166	0.354	0.268	0.99	0.76	Non-Orifice	0.170	-1.9
0.166	0.359	0.281	0.98	0.78	Non-Orifice	0.167	-0.1
0.166	0.367	0.292	0.95	0.80	Non-Orifice	0.168	-1.2
0.166	0.372	0.305	0.94	0.82	Transition Non-Orifice & Orifice	0.164	1.5
0.166	0.379	0.316	0.92	0.83	Transition Non-Orifice & Orifice	0.163	1.8
0.166	0.394	0.333	0.89	0.85	Orifice	0.162	2.9
0.166	0.429	0.366	0.82	0.85	Orifice	0.164	1.3
0.166	0.447	0.381	0.78	0.85	Orifice	0.168	-1.0

Note: G_o= 0.35 m, and all non-orifice and orifice condition correspond to a submerged-flow regime. Thus, Eqs. 2 and 4 were used to determine the discharge.

The best equation to describe all non-orifice data in free and submerged conditions was sought. The strategy was to find a relationship among flow rate, upstream depth, downstream depth, and submergence. The relationship between these variables provides a way to identify the best equation considering r^2 and SEE as selection parameters.

Various different equation forms were tested, many of which did not adequately represent the laboratory data. As a result of this analysis, a general equation (Eq. 30) was obtained, which was evaluated in different ways.

$$z = \frac{(a + bx)y + (cx + d)}{1 + (ey + f)x + (gy + h)y^2} \tag{30}$$

where x, y, and z are variables; and, a, b, c, d, e, f, g, h are parameters. A list of the equations tested is found in Table 10. The r^2 and SEE results are shown in the third and fourth columns in Table 10, and values of the parameters are found in Appendix VII.

Table 10. Six Equations Forms for Free and Submerged Non-orifice Flow

No.	Equation	r^2	SEE (m^3/s)
I	$h_u = \frac{(a + bS)Q + (cS + d)}{1 + (eQ + f)S + (gQ + h)Q^2}$	0.988	0.005
II	$h_u = \frac{(a + bh_d)Q + (ch_d + d)}{1 + (eQ + f)h_d + (gQ + h)Q^2}$	0.985	0.005
III	$h_u = \frac{(a + bQ)h_d + (cQ + d)}{1 + (eh_d + f)Q + (gh_d + h)h_d^2}$	0.982	0.006
IV	$Q = \frac{(a + bh_d)h_u + (ch_d + d)}{1 + (eh_u + f)h_d + (gh_u + h)h_u^2}$	0.991	0.004
V	$Q = \frac{(a + bh_u)h_d + (ch_u + d)}{1 + (eh_d + f)h_u + (gh_d + h)h_d^2}$	0.974	0.007
VI	$Q = \frac{(a + bS)h_u + (cS + d)}{1 + (eh_u + f)S + (gh_u + h)h_u^2}$	0.996	0.003

Table 10 shows that all equations have a high coefficient of determination, between 0.97 and 0.99, and low standard error of the estimate, between 3 and 7 l/s. After of analysis of the six equations, based on r^2 and SEE (see Fig. 31), it was determined that Eq. VI is able to model the discharge under non-orifice flow conditions (see Fig. 32). Nevertheless, this equation is only capable of fitting the laboratory data for submergences less than 0.87 with a discharge error of ±10%. The estimation of the discharge at higher submergences is less accurate than this. Equation VI has eight parameters, which are derived from the specific condition worked in the laboratory (rectangular canal, with a gate width of 0.61 m). Equation VI can be used to find the discharge in other gates, but the parameters need to be calibrated by a new site-specific condition.

Figure 33 shows the residual plot of equation VI, note that lower percentage of error for relatively low submergence and high percent error to high submergence (greater than 0.87).

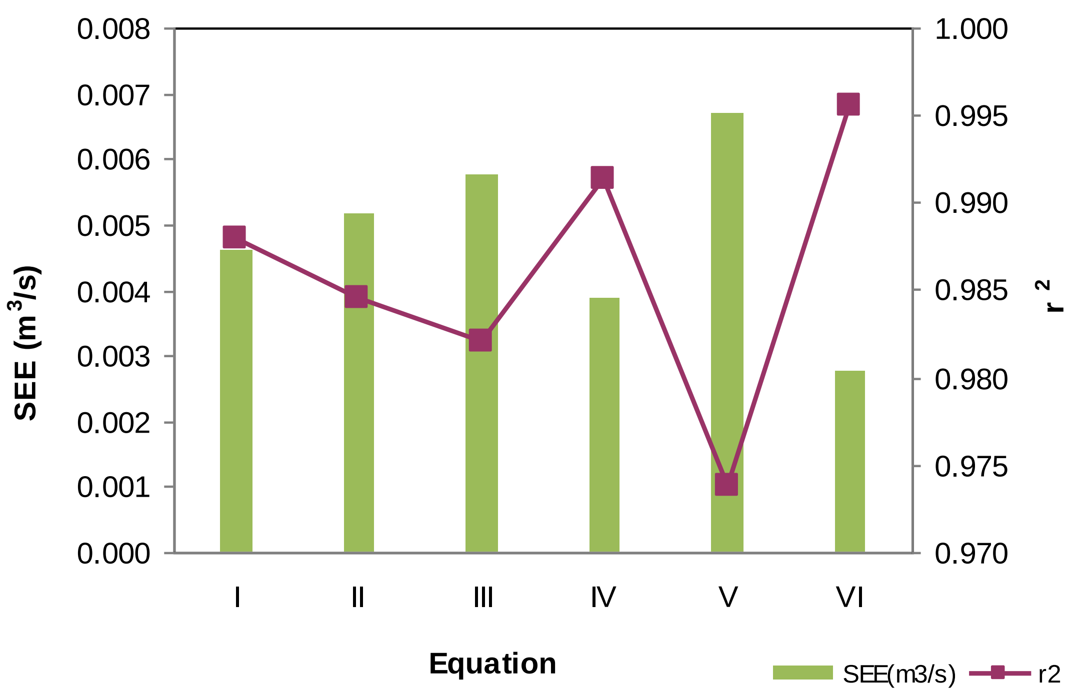

Fig. 31. SEE and r^2 values for the proposed free- and submerged non-orifice flow equations

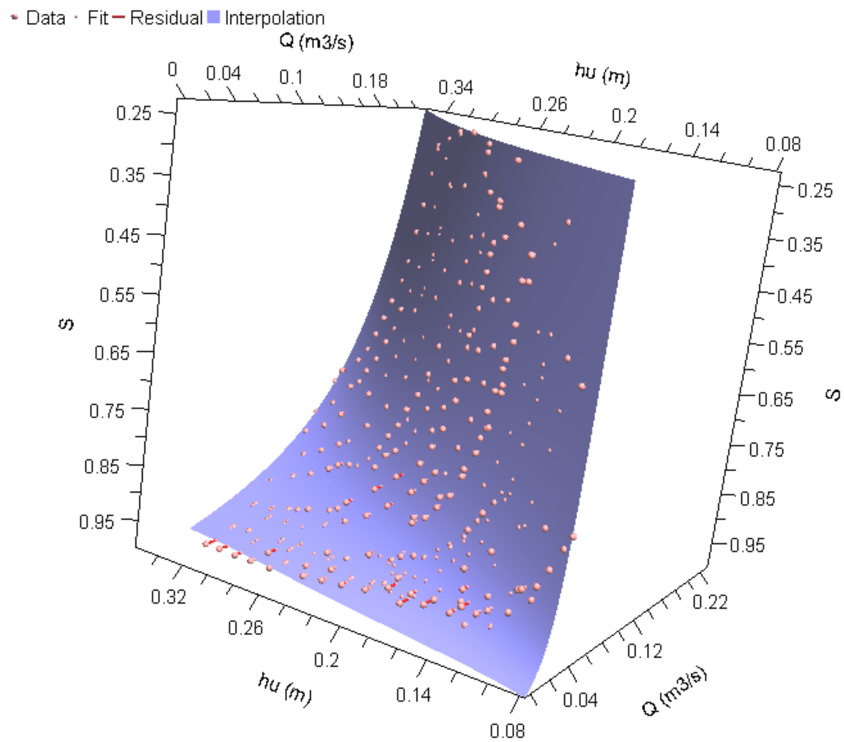

Fig. 32. Data model for Eq. VI (see Table 10)

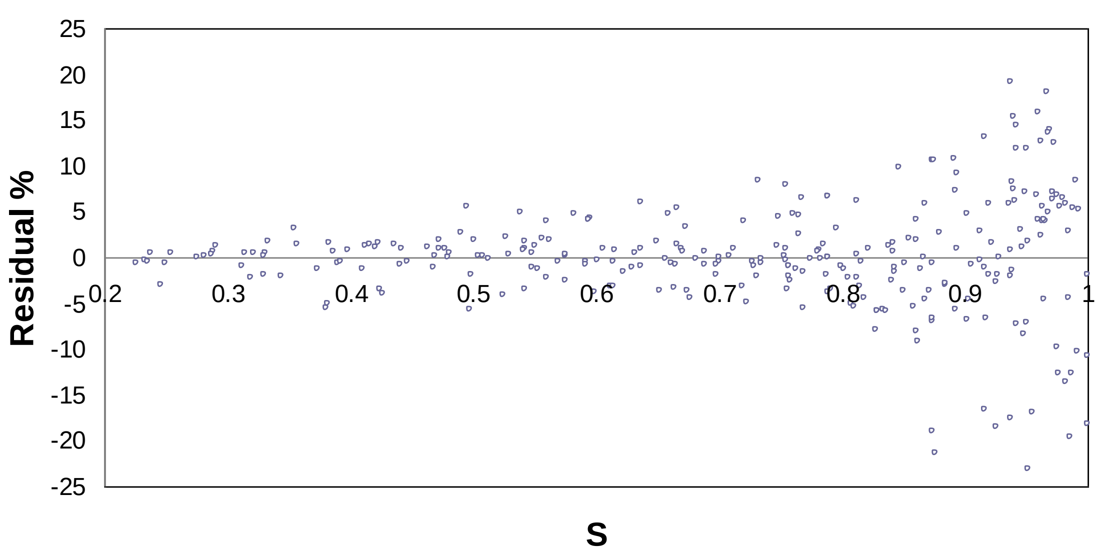

Fig.33. Submergence vs. residual percentage for Eq. VI (see Table 10)

To model the data, the proposed equation (Eq. VI) was used to calculate the discharge for non-orifice conditions, given the submergence and upstream depth. From an analysis of data non-orifice, 87% shows a percent residual lower than 10%, in the majority cases there are a good accuracy for discharges greater than 0.055 m^3/s . However, equation VI manifests the following disadvantages: a high percentage of error is shown with submergence of more than 0.87 and this equation uses eight parameters, which may cause problems of over-parameterization.

Despite the effort to develop a single equation for free and submerged flow for non-orifice conditions, none of the proposed equations provides reasonable accuracy (±5% of the true discharge). Thus, it would be necessary to conduct further research to find an equation with good estimation behavior, and also with a minimum number of required calibration parameters.

CHAPTER V

SUMMARY, CONCLUSIONS, AND RECOMMENDATIONS

Summary

The objectives of this research were to determine the value of a coefficient which defines the transition between non-orifice and orifice flow, and to determine whether a single equation could be used for free and submerged non-orifice flow through a rectangular sluice gate. To achieve this purpose, a hydraulic laboratory test was conducted in a 0.93 m-wide rectangular flume in which a vertical sluice gate was installed. The laboratory program consisted of measuring the depths upstream and downstream of the gate, for 17 different discharges from 0.02 and 0.166 m^3/s, and five different gate openings.

Three approaches were used to define the boundaries of the transition: (1) empirical equation; (2) traditional submerged non-orifice equation; and (3) specific-energy equation for open-channel flow. This latter approach was chosen to determine the limits of the transition, which were defined by two conditions: non-orifice transition threshold, and orifice transition threshold. These conditions were used to define the transition coefficient, C_o. The results of the laboratory study indicate that it is possible to know when a gate is operating in non-orifice, transitional, or orifice condition using C_o. However, when this coefficient varies between 0.83 and 1.00, it is a function of the submergence. To apply this flow regime test, it is necessary to know the gate opening and upstream and downstream water depths.

With respect to the second objective, several equations were tested, considering their coefficient of determination and standard error of the estimate to determine their accuracy. An equation to calculate the discharge for a non-orifice regime in free and submerged flow conditions was determined, given the submergence and upstream water depth. This equation provides a good correlation and good statistical parameters. However, the proposed equation does not provide reasonable accuracy (±5% of the true discharge). Thus, it would be necessary to conduct further research to find an equation with good estimation behavior.

Conclusions

There is a transition zone between non-orifice and orifice flow regimes, and it can be defined by two conditions. The first is when the gate lip initially touches in the water surface, which was defined herein as a non-orifice transition threshold, and the second condition is when upstream hydraulic seal occurs, defined as the orifice transition threshold. The following approaches were used to identify the boundaries of the transition: (1) using an empirical equation; (2) using the traditional submerged non-orifice equation; and (3) using the specific-energy equation. The latter approach was chosen to define the boundaries of the transition since it is simple, and because there is a good agreement between the laboratory observations and the calculated values.

A simple method to define the boundaries of the transition regime between non-orifice and orifice flow regimes through a vertical sluice gate was developed. It is based on the specific-energy equation and consists in determining the non-orifice and orifice transition thresholds. The results indicate that Eqs. 19 and 22 can adequately predict the threshold of flow regime change. These thresholds must be compared with the gate setting to define the limits of the transition.

A dimensionless parameter that measures the ratio of gate opening and upstream water depth was used to determine whether the gate is operating under orifice or non-orifice conditions. It was defined as transition coefficient, C_o. The experimental results show that C_o greater than 1.00 indicates non-orifice flow, and C_o lower than 0.83 corresponds to orifice flow. To define the regime in a range of C_o between 0.83 and 1.00 it is necessary to consider the submergence, S. Figure 29 provides a way to identify which regime will occur in the range between 0.83 and 1.00.

The analysis conducted to determine whether a single equation can be used for free and submerged non-orifice flow through the gate showed that from six equations proposed, Eq. VI, provides a good correlation and good statistical parameters. However, this equation does not give reasonable accuracy for submergences greater than 87% and traditional equations forms can fit the data even better than Eq. VI. Thus, despite the effort to develop a single equation for free and submerged flow for non-orifice conditions, none of the proposed equations provides reasonable accuracy (±5% of the true discharge).

Recommendations

This study used a flume and a vertical sluice gate with specific characteristics (e.g. rectangular canal, gate width of 0.61 m) and with specific conditions (e.g. range of flow rate from 0.2 m^3/s to 0.166 m^3/s, for five specific gate openings). In order to obtain a better understanding of the behavior of the transition regime, it is recommendable to make similar experiments with other types of gates, different ratios of gate width to channel width, and different discharge ranges.

More testing data should be pursued in the transition regime, using accurate instruments, which can provide precise measurements to determine whether the transition non-orifice and orifice has the same or different behavior than that reported in this research. Considering that there is a transition zone between orifice and non-orifice regimes, behavior of the discharge in this specific zone should be analyzed.

Efforts should be made to develop a unique non-orifice flow equation that can describe the relationship among discharge, submergence, and water depths, avoiding the need to use two equations (free and submerged) and this proposed equation should be analyzed under non-laboratory conditions to see the different variables, which can affect the equation. The proposed equation should provide not only good estimation behavior, but be as simple a formula as possible.

REFERENCES

Ames, G.O. (1999). “Submerged flow at open channel gate”. Unpublished M.S. thesis, Utah State Univ. , Logan, UT.

Clemmens, A.J. Strelkoff, T. S., and Replogle, J. A. (2003). “Calibration of submerged radial gates”. J. Hydraul. Eng., ASCE, 129(9), 680-687.

Garbrecht, G. (1977). Discussion on “Discharge computation at river control structures”. J Hydr. Div., ASCE. 103(HY12), 1481-1484.

Hadi, H.J. (2003). “High resolution methods for flow regime transitions at canal structures”. Unpublished PhD dissertation, Utah State Univ., Logan, UT.

Jeppson, R. (2001). *Open-channel flow utilizing computers*. Utah State Univ., Utah, UT.

Merkley, G.P. (2006a). “Irrigation conveyance and control: Flow measurement and structure design”. Lecture notes, Biological and Irrigation Engineering Dept., Utah State Univ., Logan, UT.

Merkley, G. P. (2006b). *RootCanal hydraulic simulation model, user’s guide and technical reference*. Version 1.00q, BIE Dept., Utah State Univ., Logan, UT.

Miller, W. R. (1996). *Flow measurement engineering handbook* (3rd ed.), McGraw-Hill, Boston, MA.

Nguyen, C.C. (2000). “Hydraulic analysis of unsteady flow in open channels with changing flow regimes at a gate structure”, Utah State Univ., Logan, UT.

Torres, A.F. (2006). “Analysis of transition submergence and hysteresis effects in a 3-ft cutthroat flume”. Unpublished M.S. thesis, Utah State Univ., Logan, UT.

Wahl, T.L. (2004). “Issues and problems with calibration of canal gates”. World Water & Environmental Resources Congress, Salt Lake City, UT.

APPENDICES

Appendix I. Vertical Sluice Gate Design Drawings, Construction, and Installation

Gate Design (All measure are in metric units)

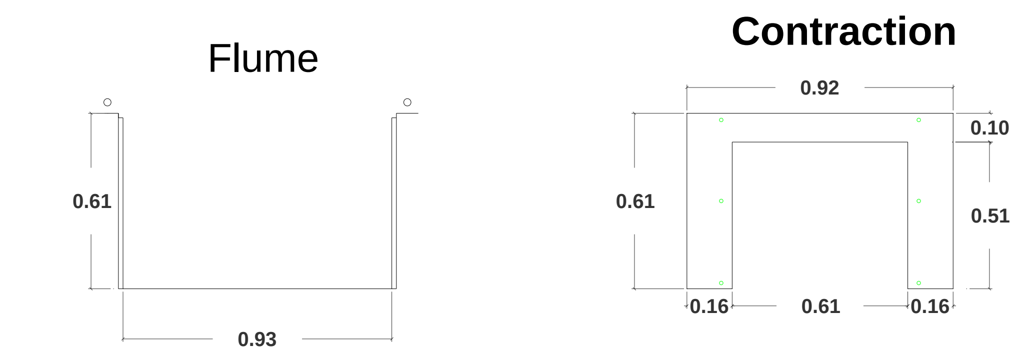

Fig. 34. Flume and gate dimensions

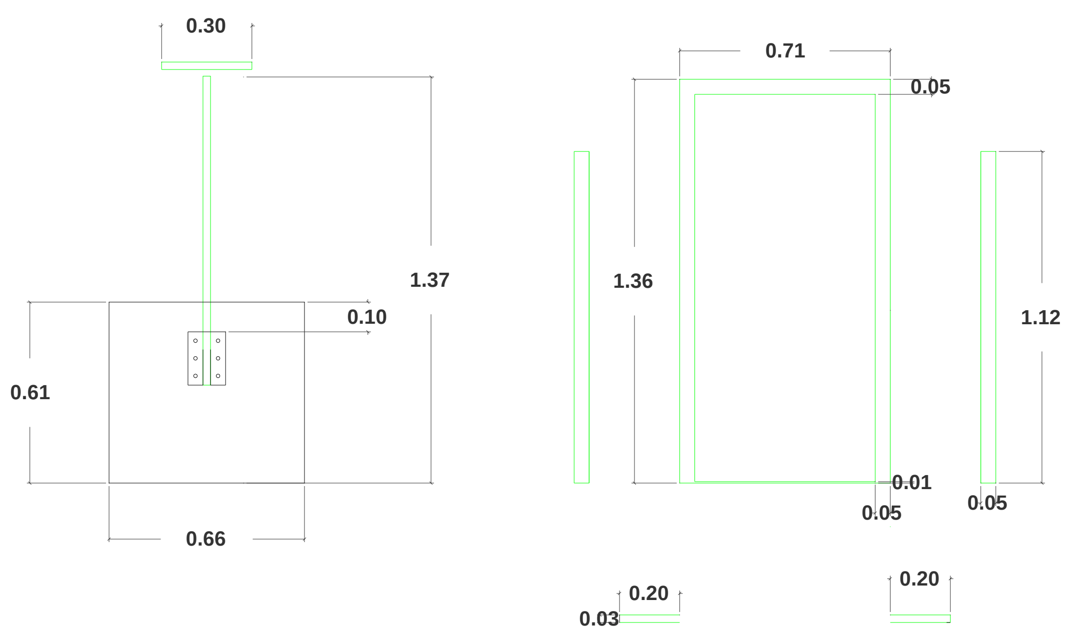

Fig. 35. Vertical sluice gate structure dimensions

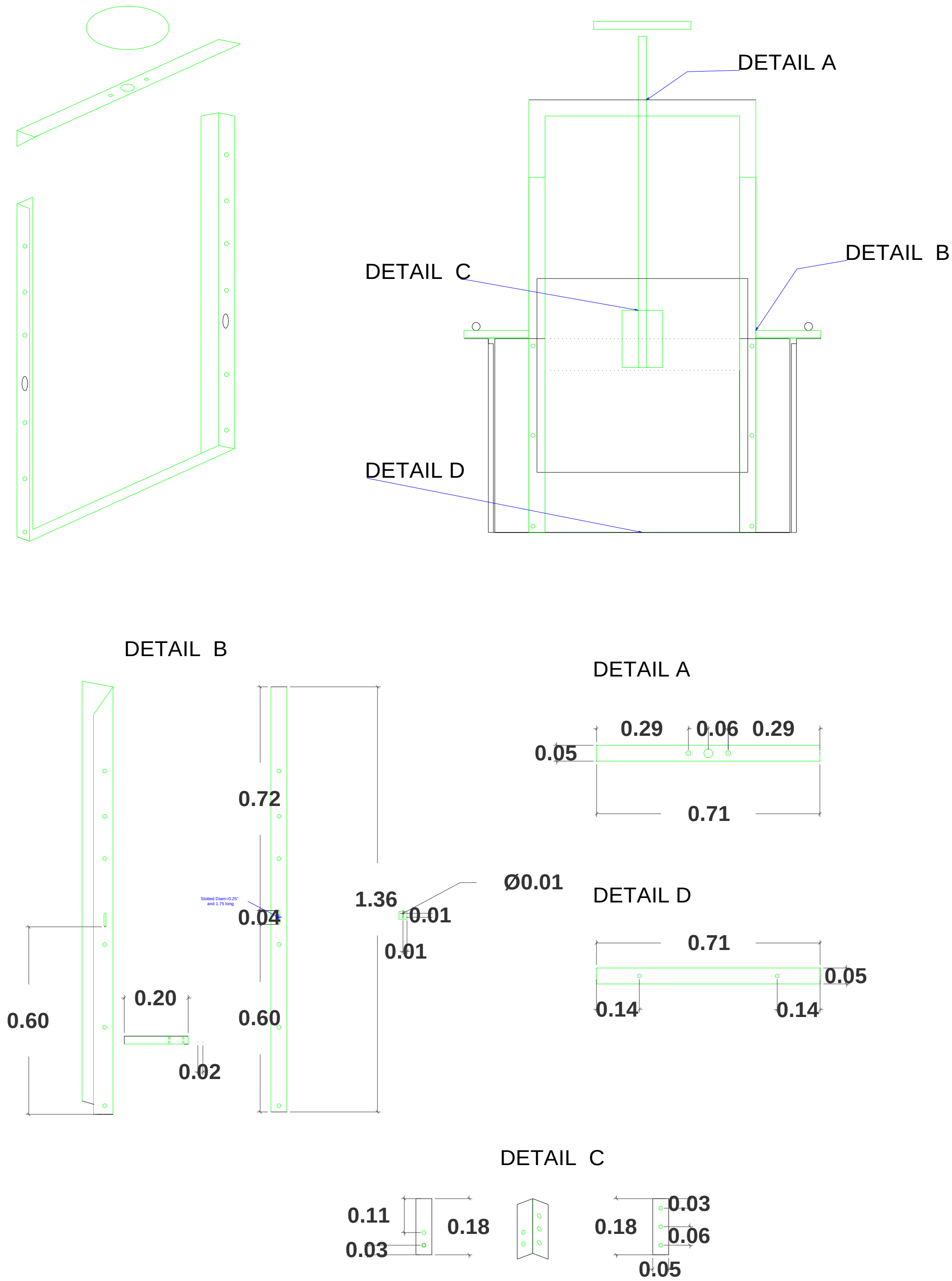

Fig. 36. Gate structure details

The following sequence photos illustrate the construction of the gate:

Fig.37. Construction of the vertical sluice gate

Fig.38. Cutting the acrylic to make the gate face

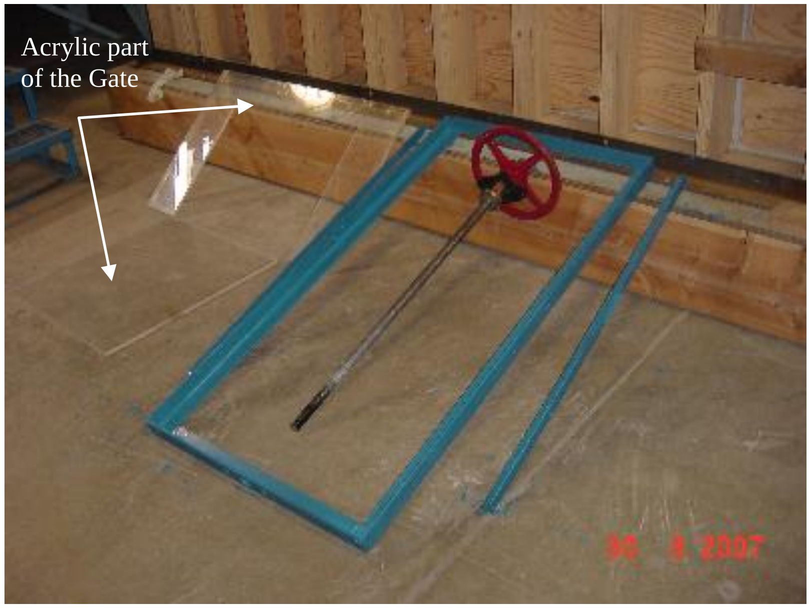

Fig. 39. Parts of the gate before to installation in the flume

Fig.40. Gate after installation in the rectangular flume

Appendix II. Details of the Flow Measurement Equations

Appendix II

To calculate the flow rate of the pipe in the flume used in laboratory was necessary calibrations to define the coefficient of discharge, C_d. The following equations were used:

C_d equation (4-inch pipe with orifice plate):

$$C_d = 5.336(10)^{-33}R_e^6 - 4.752(10)^{-27}R_e^5 + 1.692(10)^{-21}R_e^4 \\ -3.088(10)^{-16}R_e^3 + 3.067(10)^{-11}R_e^2 - 1.640(10)^{-6}R_e + 0.664 \tag{31}$$

C_d equation (12-inch pipe with orifice plate):

$$C_d = 1.184(10)^{-36}R_e^6 - 4.957(10)^{-30}R_e^5 + 7.119(10)^{-24}R_e^4 - \\ 4.766(10)^{-18}R_e^3 + 1.592(10)^{-12}R_e^2 - 2.575(10)^{-7}R_e + 0.628 \tag{32}$$

in which R_e is the Reynolds number, which is defined as:

$$R_e = \frac{VD}{\nu} \tag{33}$$

where V is mean velocity (ft/s) of flow in the pipe at a cross section; and, ν is the kinematic viscosity of water (ft^2/s), which is a function of the water temperature.

Appendix. III. Laboratory Data Form

Appendix. III

Laboratory Data Form

Rectangular Canal Gate Laboratory Data Sheet
Omar Alminagorta -- 2007

Date:		Sheet:	
Start time:		Temperature:	
End time:			
Supply Pipe:	4"	Fluid:	Blue
	12"		Mercury

		Water Manometer Readings (cm)				Manometer Blue/Hg		Position Tailgate	Flow Condition	Hydralic Jump	Comments
Trial	G_o	Downstream		Upstream		left	right				
	(cm)	Outer	Inner	Inner	Outer	(cm)	(cm)	(Number of turns)	(Orifice/Non Orif)	(yes/no)	
1											
2											
3											
4											
5											
6											
7											
8											
9											
10											
11											
12											
13											
14											
15											
16											
17											
18											
19											
20											

Appendix. IV. Laboratory Data

Table 11. Laboratory Data for a Gate Opening of 0.15 m

Q (m^3/s)	S	h_u (m)	Gate Status
0.020	0.789	0.081	Non-Orifice
0.020	0.829	0.088	Non-Orifice
0.020	0.861	0.094	Non-Orifice
0.020	0.873	0.103	Non-Orifice
0.020	0.917	0.109	Non-Orifice
0.020	0.949	0.118	Non-Orifice
0.020	0.963	0.135	Non-Orifice
0.020	0.961	0.153	Transition Non-Orifice & Orifice
0.020	0.956	0.160	Orifice
0.020	0.953	0.169	Orifice
0.020	0.952	0.177	Orifice
0.020	0.959	0.194	Orifice
0.020	0.973	0.224	Orifice
0.020	0.978	0.269	Orifice
0.020	0.987	0.308	Orifice
0.020	0.986	0.348	Orifice
0.020	0.987	0.379	Orifice
0.020	0.993	0.408	Orifice
0.027	0.542	0.090	Non-Orifice
0.027	0.775	0.098	Non-Orifice
0.027	0.892	0.112	Non-Orifice
0.027	0.913	0.127	Non-Orifice
0.027	0.937	0.144	Non-Orifice
0.027	0.963	0.162	Transition Non-Orifice & Orifice
0.027	0.949	0.197	Orifice
0.027	0.968	0.247	Orifice
0.027	0.970	0.331	Orifice
0.027	0.980	0.400	Orifice
0.035	0.512	0.105	Non-Orifice
0.035	0.659	0.106	Non-Orifice
0.035	0.749	0.112	Non-Orifice
0.035	0.796	0.118	Non-Orifice
0.035	0.850	0.134	Non-Orifice
0.035	0.893	0.150	Non-Orifice
0.035	0.943	0.158	Transition Non-Orifice & Orifice
0.035	0.944	0.161	Transition Non-Orifice & Orifice
0.035	0.933	0.165	Orifice
0.035	0.928	0.168	Orifice
0.035	0.926	0.176	Orifice
0.035	0.923	0.194	Orifice
0.035	0.943	0.227	Orifice
0.035	0.946	0.276	Orifice
0.035	0.956	0.319	Orifice
0.035	0.961	0.358	Orifice
0.035	0.960	0.396	Orifice
0.035	0.965	0.426	Orifice
0.045	0.490	0.122	Non-Orifice
0.045	0.595	0.124	Non-Orifice
0.045	0.673	0.129	Non-Orifice
0.045	0.768	0.134	Non-Orifice
0.045	0.781	0.142	Non-Orifice
0.045	0.805	0.149	Non-Orifice
0.045	0.840	0.157	Non-Orifice
0.045	0.849	0.159	Transition Non-Orifice & Orifice
0.045	0.846	0.163	Transition Non-Orifice & Orifice
0.045	0.861	0.166	Transition Non-Orifice & Orifice
0.045	0.864	0.169	Orifice
0.045	0.872	0.172	Orifice
0.045	0.880	0.175	Orifice
0.045	0.876	0.178	Orifice
0.045	0.871	0.187	Orifice
0.045	0.883	0.205	Orifice
0.045	0.903	0.238	Orifice
0.045	0.919	0.286	Orifice
0.045	0.928	0.332	Orifice
0.045	0.933	0.372	Orifice
0.045	0.944	0.409	Orifice
0.045	0.947	0.432	Orifice
0.046	0.315	0.123	Non-Orifice
0.046	0.539	0.124	Non-Orifice
0.046	0.637	0.127	Non-Orifice
0.046	0.732	0.131	Non-Orifice
0.046	0.760	0.138	Non-Orifice
0.046	0.812	0.144	Non-Orifice
0.046	0.822	0.152	Non-Orifice
0.046	0.860	0.158	Non-Orifice
0.046	0.877	0.163	Transition Non-Orifice & Orifice
0.046	0.872	0.165	Orifice
0.046	0.887	0.212	Orifice
0.046	0.916	0.297	Orifice
0.046	0.933	0.367	Orifice
0.046	0.941	0.404	Orifice
0.051	0.354	0.132	Non-Orifice
0.051	0.495	0.133	Non-Orifice
0.051	0.583	0.137	Non-Orifice
0.051	0.666	0.141	Non-Orifice
0.051	0.720	0.147	Non-Orifice
0.051	0.766	0.154	Non-Orifice
0.051	0.801	0.161	Transition Non-Orifice & Orifice
0.051	0.828	0.169	Transition Non-Orifice & Orifice
0.051	0.860	0.179	Orifice
0.051	0.856	0.209	Orifice
0.051	0.877	0.244	Orifice
0.051	0.907	0.292	Orifice
0.051	0.914	0.339	Orifice
0.051	0.924	0.407	Orifice
0.051	0.930	0.430	Orifice
0.055	0.382	0.148	Non-Orifice
0.055	0.424	0.148	Non-Orifice
0.055	0.497	0.152	Non-Orifice
0.055	0.599	0.155	Non-Orifice
0.055	0.676	0.161	Non-Orifice
0.055	0.721	0.165	Transition Non-Orifice & Orifice
0.055	0.715	0.169	Transition Non-Orifice & Orifice
0.055	0.759	0.172	Transition Non-Orifice & Orifice
0.055	0.770	0.174	Orifice
0.055	0.785	0.177	Orifice
0.055	0.798	0.179	Orifice
0.055	0.797	0.183	Orifice
0.055	0.817	0.186	Orifice
0.055	0.804	0.196	Orifice
0.055	0.783	0.208	Orifice
0.055	0.785	0.219	Orifice
0.055	0.792	0.228	Orifice
0.055	0.797	0.237	Orifice
0.055	0.803	0.249	Orifice
0.055	0.819	0.265	Orifice

Q (m^3/s)	S	h_u (m)	Gate Status
0.055	0.825	0.283	Orifice
0.055	0.845	0.317	Orifice
0.055	0.862	0.347	Orifice
0.055	0.874	0.390	Orifice
0.055	0.884	0.432	Orifice
0.058	0.427	0.154	Non-Orifice
0.058	0.559	0.157	Non-Orifice
0.058	0.614	0.161	Non-Orifice
0.058	0.698	0.166	Non-Orifice
0.058	0.733	0.173	Transition Non-Orifice & Orifice
0.058	0.759	0.175	Transition Non-Orifice & Orifice
0.058	0.765	0.179	Orifice
0.058	0.769	0.182	Orifice
0.058	0.788	0.184	Orifice
0.058	0.799	0.194	Orifice
0.058	0.778	0.205	Orifice
0.058	0.770	0.218	Orifice
0.058	0.776	0.228	Orifice
0.058	0.789	0.247	Orifice
0.058	0.812	0.283	Orifice
0.058	0.833	0.317	Orifice
0.058	0.848	0.349	Orifice
0.058	0.865	0.393	Orifice
0.058	0.875	0.434	Orifice
0.066	0.344	0.165	Non-Orifice
0.066	0.543	0.169	Transition Non-Orifice & Orifice
0.066	0.681	0.182	Transition Non-Orifice & Orifice
0.066	0.752	0.198	Orifice
0.066	0.732	0.224	Orifice
0.066	0.748	0.262	Orifice
0.066	0.794	0.316	Orifice
0.066	0.817	0.366	Orifice
0.066	0.842	0.450	Orifice

Table 12. Laboratory Data for a Gate Opening of 0.20 m

Q (m^3/s)	S	h_u (m)	Gate Status
0.020	0.765	0.077	Non-Orifice
0.020	0.789	0.081	Non-Orifice
0.020	0.829	0.088	Non-Orifice
0.020	0.885	0.096	Non-Orifice
0.020	0.876	0.105	Non-Orifice
0.020	0.926	0.122	Non-Orifice
0.020	0.938	0.129	Non-Orifice
0.020	0.935	0.139	Non-Orifice
0.020	0.952	0.146	Non-Orifice
0.020	0.954	0.164	Non-Orifice
0.020	0.967	0.180	Non-Orifice
0.020	0.990	0.197	Transition Non-Orifice & Orifice
0.020	0.982	0.198	Transition Non-Orifice & Orifice
0.020	0.985	0.207	Orifice
0.020	0.982	0.221	Orifice
0.020	0.982	0.252	Orifice
0.020	0.986	0.293	Orifice
0.020	0.991	0.329	Orifice
0.020	0.992	0.367	Orifice
0.020	0.992	0.398	Orifice
0.020	0.993	0.417	Orifice
0.035	0.595	0.104	Non-Orifice
0.035	0.789	0.114	Non-Orifice
0.035	0.868	0.129	Non-Orifice
0.035	0.938	0.162	Non-Orifice
0.035	0.960	0.177	Non-Orifice
0.035	0.967	0.185	Non-Orifice
0.035	0.969	0.194	Non-Orifice
0.035	0.975	0.202	Transition Non-Orifice & Orifice
0.035	0.975	0.204	Transition Non-Orifice & Orifice
0.035	0.973	0.207	Orifice
0.035	0.976	0.209	Orifice
0.035	0.972	0.212	Orifice
0.035	0.972	0.214	Orifice
0.035	0.973	0.224	Orifice
0.035	0.975	0.240	Orifice
0.035	0.970	0.271	Orifice
0.035	0.974	0.314	Orifice
0.035	0.983	0.354	Orifice
0.035	0.982	0.391	Orifice

Q (m^3/s)	S	h_u (m)	Gate Status
0.035	0.981	0.421	Orifice
0.045	0.560	0.123	Non-Orifice
0.045	0.755	0.131	Non-Orifice
0.045	0.847	0.144	Non-Orifice
0.045	0.874	0.151	Non-Orifice
0.045	0.894	0.161	Non-Orifice
0.045	0.916	0.168	Non-Orifice
0.045	0.937	0.175	Non-Orifice
0.045	0.940	0.184	Non-Orifice
0.045	0.943	0.192	Non-Orifice
0.045	0.950	0.201	Non-Orifice
0.045	0.961	0.207	Transition Non-Orifice & Orifice
0.045	0.958	0.217	Transition Non-Orifice & Orifice
0.045	0.964	0.224	Orifice
0.045	0.961	0.233	Orifice
0.045	0.955	0.243	Orifice
0.045	0.960	0.251	Orifice
0.045	0.959	0.267	Orifice
0.045	0.961	0.312	Orifice
0.045	0.966	0.354	Orifice
0.045	0.969	0.392	Orifice
0.045	0.967	0.425	Orifice
0.046	0.315	0.123	Non-Orifice
0.046	0.539	0.124	Non-Orifice
0.046	0.637	0.127	Non-Orifice
0.046	0.732	0.131	Non-Orifice
0.046	0.760	0.138	Non-Orifice
0.046	0.812	0.144	Non-Orifice
0.046	0.822	0.152	Non-Orifice
0.046	0.855	0.159	Non-Orifice
0.046	0.880	0.167	Non-Orifice
0.046	0.903	0.175	Non-Orifice
0.046	0.913	0.184	Non-Orifice
0.046	0.916	0.192	Non-Orifice
0.046	0.925	0.201	Non-Orifice
0.046	0.941	0.203	Non-Orifice
0.046	0.951	0.204	Transition Non-Orifice & Orifice
0.046	0.953	0.214	Orifice
0.046	0.951	0.264	Orifice
0.046	0.963	0.351	Orifice

Q (m^3/s)	S	h_u (m)	Gate Status
0.046	0.969	0.387	Orifice
0.046	0.966	0.444	Orifice
0.051	0.354	0.132	Non-Orifice
0.051	0.495	0.133	Non-Orifice
0.051	0.583	0.137	Non-Orifice
0.051	0.666	0.141	Non-Orifice
0.051	0.720	0.147	Non-Orifice
0.051	0.766	0.154	Non-Orifice
0.051	0.801	0.161	Non-Orifice
0.051	0.875	0.169	Non-Orifice
0.051	0.892	0.176	Non-Orifice
0.051	0.920	0.201	Non-Orifice
0.051	0.928	0.209	Transition Non-Orifice & Orifice
0.051	0.940	0.217	Orifice
0.051	0.938	0.243	Orifice
0.051	0.946	0.276	Orifice
0.051	0.950	0.322	Orifice
0.051	0.959	0.388	Orifice
0.051	0.960	0.424	Orifice
0.055	0.381	0.149	Non-Orifice
0.055	0.525	0.152	Non-Orifice
0.055	0.612	0.155	Non-Orifice
0.055	0.674	0.160	Non-Orifice
0.055	0.722	0.166	Non-Orifice
0.055	0.768	0.173	Non-Orifice
0.055	0.807	0.179	Non-Orifice
0.055	0.834	0.187	Non-Orifice
0.055	0.858	0.194	Non-Orifice
0.055	0.874	0.203	Non-Orifice
0.055	0.900	0.210	Transition Non-Orifice & Orifice
0.055	0.897	0.213	Transition Non-Orifice & Orifice
0.055	0.905	0.221	Orifice
0.055	0.905	0.231	Orifice
0.055	0.906	0.250	Orifice
0.055	0.910	0.267	Orifice
0.055	0.915	0.283	Orifice
0.055	0.921	0.331	Orifice
0.055	0.933	0.374	Orifice
0.055	0.933	0.413	Orifice
0.058	0.499	0.154	Non-Orifice

Q (m^3/s)	S	h_u (m)	Gate Status
0.058	0.575	0.158	Non-Orifice
0.058	0.652	0.164	Non-Orifice
0.058	0.758	0.174	Non-Orifice
0.058	0.819	0.188	Non-Orifice
0.058	0.867	0.204	Non-Orifice
0.058	0.886	0.211	Transition Non-Orifice & Orifice
0.058	0.883	0.214	Transition Non-Orifice & Orifice
0.058	0.904	0.219	Orifice
0.058	0.909	0.230	Orifice
0.058	0.912	0.238	Orifice
0.058	0.899	0.249	Orifice
0.058	0.906	0.266	Orifice
0.058	0.908	0.283	Orifice
0.058	0.916	0.332	Orifice
0.058	0.928	0.375	Orifice
0.058	0.927	0.414	Orifice
0.075	0.245	0.178	Non-Orifice
0.075	0.373	0.179	Non-Orifice
0.075	0.480	0.181	Non-Orifice
0.075	0.569	0.186	Non-Orifice
0.075	0.622	0.191	Non-Orifice
0.075	0.664	0.197	Non-Orifice
0.075	0.719	0.203	Non-Orifice
0.075	0.756	0.209	Non-Orifice
0.075	0.777	0.216	Transition Non-Orifice & Orifice
0.075	0.799	0.224	Transition Non-Orifice & Orifice
0.075	0.841	0.233	Orifice
0.075	0.852	0.243	Orifice
0.075	0.854	0.254	Orifice
0.075	0.860	0.271	Orifice
0.075	0.866	0.306	Orifice
0.075	0.871	0.357	Orifice
0.075	0.892	0.443	Orifice
0.082	0.319	0.190	Non-Orifice
0.082	0.329	0.190	Non-Orifice
0.082	0.390	0.190	Non-Orifice
0.082	0.410	0.192	Non-Orifice
0.082	0.440	0.192	Non-Orifice
0.082	0.468	0.194	Non-Orifice
0.082	0.504	0.194	Non-Orifice

Q (m^3/s)	S	h_u (m)	Gate Status
0.082	0.543	0.195	Non-Orifice
0.082	0.553	0.198	Non-Orifice
0.082	0.575	0.198	Non-Orifice
0.082	0.637	0.204	Non-Orifice
0.082	0.688	0.209	Non-Orifice
0.082	0.734	0.215	Non-Orifice
0.082	0.764	0.221	Transition Non-Orifice & Orifice
0.082	0.772	0.224	Orifice
0.082	0.763	0.228	Orifice
0.082	0.782	0.230	Orifice
0.082	0.781	0.233	Orifice
0.082	0.818	0.242	Orifice
0.082	0.809	0.252	Orifice
0.082	0.812	0.272	Orifice
0.082	0.818	0.292	Orifice
0.082	0.835	0.346	Orifice
0.082	0.847	0.379	Orifice
0.082	0.858	0.408	Orifice
0.082	0.867	0.436	Orifice
0.082	0.873	0.449	Orifice
0.100	0.250	0.215	Non-Orifice
0.100	0.357	0.215	Non-Orifice
0.100	0.442	0.219	Non-Orifice
0.100	0.519	0.223	Transition Non-Orifice & Orifice
0.100	0.567	0.229	Transition Non-Orifice & Orifice
0.100	0.577	0.232	Transition Non-Orifice & Orifice
0.100	0.593	0.234	Orifice
0.100	0.618	0.236	Orifice
0.100	0.623	0.239	Orifice
0.100	0.651	0.247	Orifice
0.100	0.712	0.254	Orifice
0.100	0.715	0.260	Orifice
0.100	0.723	0.271	Orifice
0.100	0.721	0.284	Orifice
0.100	0.728	0.295	Orifice
0.100	0.743	0.315	Orifice
0.100	0.760	0.354	Orifice
0.100	0.779	0.390	Orifice
0.100	0.788	0.424	Orifice
0.100	0.803	0.453	Orifice

Table 13. Laboratory Data for a Gate Opening of 0.25 m

Q (m^3/s)	S	h_u (m)	Gate Status
0.027	0.542	0.090	Non-Orifice
0.027	0.775	0.098	Non-Orifice
0.027	0.892	0.112	Non-Orifice
0.027	0.913	0.127	Non-Orifice
0.027	0.916	0.144	Non-Orifice
0.027	0.950	0.162	Non-Orifice
0.027	0.955	0.178	Non-Orifice
0.027	0.959	0.194	Non-Orifice
0.027	0.976	0.210	Non-Orifice
0.027	0.982	0.227	Non-Orifice
0.027	0.988	0.242	Non-Orifice
0.027	0.992	0.257	Transition Non-Orifice & Orifice
0.027	0.992	0.362	Orifice
0.027	0.992	0.396	Orifice
0.035	0.595	0.104	Non-Orifice
0.035	0.789	0.114	Non-Orifice
0.035	0.948	0.194	Non-Orifice
0.035	0.965	0.202	Non-Orifice
0.035	0.971	0.210	Non-Orifice
0.035	0.978	0.226	Non-Orifice
0.035	0.975	0.242	Non-Orifice
0.035	0.982	0.249	Transition Non-Orifice & Orifice
0.035	0.988	0.256	Orifice
0.035	0.989	0.271	Orifice
0.035	0.982	0.301	Orifice
0.035	0.985	0.340	Orifice
0.035	0.984	0.378	Orifice
0.035	0.988	0.410	Orifice
0.046	0.315	0.123	Non-Orifice
0.046	0.539	0.124	Non-Orifice
0.046	0.637	0.127	Non-Orifice
0.046	0.732	0.131	Non-Orifice
0.046	0.760	0.138	Non-Orifice
0.046	0.812	0.144	Non-Orifice
0.046	0.822	0.152	Non-Orifice
0.046	0.855	0.159	Non-Orifice
0.046	0.880	0.167	Non-Orifice
0.046	0.903	0.175	Non-Orifice
0.046	0.913	0.184	Non-Orifice
0.046	0.916	0.192	Non-Orifice

Q (m^3/s)	S	h_u (m)	Gate Status
0.046	0.925	0.201	Non-Orifice
0.046	0.937	0.207	Non-Orifice
0.046	0.942	0.224	Non-Orifice
0.046	0.962	0.239	Non-Orifice
0.046	0.972	0.251	Non-Orifice
0.046	0.968	0.253	Transition Non-Orifice & Orifice
0.046	0.969	0.262	Orifice
0.046	0.974	0.307	Orifice
0.046	0.978	0.370	Orifice
0.046	0.981	0.427	Orifice
0.051	0.354	0.132	Non-Orifice
0.051	0.495	0.133	Non-Orifice
0.051	0.583	0.137	Non-Orifice
0.051	0.666	0.141	Non-Orifice
0.051	0.720	0.147	Non-Orifice
0.051	0.766	0.154	Non-Orifice
0.051	0.801	0.161	Non-Orifice
0.051	0.875	0.169	Non-Orifice
0.051	0.892	0.176	Non-Orifice
0.051	0.920	0.201	Non-Orifice
0.051	0.942	0.208	Non-Orifice
0.051	0.940	0.217	Non-Orifice
0.051	0.962	0.240	Non-Orifice
0.051	0.968	0.249	Non-Orifice
0.051	0.969	0.256	Transition Non-Orifice & Orifice
0.051	0.973	0.263	Orifice
0.051	0.975	0.278	Orifice
0.051	0.980	0.308	Orifice
0.051	0.972	0.352	Orifice
0.051	0.976	0.414	Orifice
0.066	0.344	0.165	Non-Orifice
0.066	0.469	0.166	Non-Orifice
0.066	0.549	0.171	Non-Orifice
0.066	0.614	0.174	Non-Orifice
0.066	0.681	0.179	Non-Orifice
0.066	0.735	0.185	Non-Orifice
0.066	0.785	0.191	Non-Orifice
0.066	0.789	0.199	Non-Orifice
0.066	0.810	0.206	Non-Orifice
0.066	0.836	0.214	Non-Orifice

Q (m^3/s)	S	h_u (m)	Gate Status
0.066	0.874	0.230	Non-Orifice
0.066	0.904	0.244	Non-Orifice
0.066	0.927	0.261	Transition Non-Orifice & Orifice
0.066	0.935	0.277	Orifice
0.066	0.941	0.325	Orifice
0.066	0.946	0.369	Orifice
0.066	0.949	0.409	Orifice
0.066	0.952	0.434	Orifice
0.075	0.245	0.178	Non-Orifice
0.075	0.373	0.179	Non-Orifice
0.075	0.480	0.181	Non-Orifice
0.075	0.569	0.186	Non-Orifice
0.075	0.612	0.191	Non-Orifice
0.075	0.654	0.197	Non-Orifice
0.075	0.719	0.203	Non-Orifice
0.075	0.756	0.209	Non-Orifice
0.075	0.791	0.216	Non-Orifice
0.075	0.827	0.232	Non-Orifice
0.075	0.862	0.247	Non-Orifice
0.075	0.903	0.259	Transition Non-Orifice & Orifice
0.075	0.914	0.267	Orifice
0.075	0.917	0.276	Orifice
0.075	0.918	0.294	Orifice
0.075	0.926	0.326	Orifice
0.075	0.925	0.374	Orifice
0.075	0.934	0.441	Orifice
0.091	0.312	0.204	Non-Orifice
0.091	0.386	0.204	Non-Orifice
0.091	0.416	0.204	Non-Orifice
0.091	0.472	0.207	Non-Orifice
0.091	0.556	0.210	Non-Orifice
0.091	0.615	0.216	Non-Orifice
0.091	0.669	0.221	Non-Orifice
0.091	0.709	0.227	Non-Orifice
0.091	0.755	0.233	Non-Orifice
0.091	0.782	0.239	Non-Orifice
0.091	0.801	0.247	Non-Orifice
0.091	0.815	0.254	Non-Orifice
0.091	0.843	0.261	Non-Orifice
0.091	0.854	0.268	Transition Non-Orifice & Orifice

Q (m^3/s)	S	h_u (m)	Gate Status
0.091	0.872	0.270	Transition Non-Orifice & Orifice
0.091	0.868	0.273	Transition Non-Orifice & Orifice
0.091	0.877	0.276	Transition Non-Orifice & Orifice
0.091	0.878	0.279	Orifice
0.091	0.879	0.282	Orifice
0.091	0.880	0.291	Orifice
0.091	0.877	0.302	Orifice
0.091	0.877	0.310	Orifice
0.091	0.881	0.328	Orifice
0.091	0.884	0.362	Orifice
0.091	0.888	0.394	Orifice
0.091	0.895	0.421	Orifice
0.100	0.288	0.214	Non-Orifice
0.100	0.562	0.224	Non-Orifice
0.100	0.666	0.234	Non-Orifice
0.100	0.748	0.246	Non-Orifice
0.100	0.788	0.260	Non-Orifice
0.100	0.820	0.267	Transition Non-Orifice & Orifice
0.100	0.836	0.274	Orifice
0.100	0.847	0.282	Orifice
0.100	0.853	0.292	Orifice
0.100	0.854	0.302	Orifice
0.100	0.858	0.310	Orifice
0.100	0.859	0.348	Orifice
0.100	0.869	0.397	Orifice
0.100	0.878	0.426	Orifice
0.100	0.236	0.215	Non-Orifice
0.100	0.287	0.215	Non-Orifice
0.100	0.398	0.218	Non-Orifice
0.100	0.481	0.222	Non-Orifice
0.100	0.541	0.225	Non-Orifice
0.100	0.601	0.231	Non-Orifice
0.100	0.656	0.236	Non-Orifice
0.100	0.698	0.242	Non-Orifice
0.100	0.730	0.249	Non-Orifice
0.100	0.763	0.254	Non-Orifice
0.100	0.816	0.266	Non-Orifice
0.100	0.821	0.268	Transition Non-Orifice & Orifice
0.100	0.845	0.284	Orifice
0.100	0.857	0.302	Orifice

Q (m^3/s)	S	h_u (m)	Gate Status
0.100	0.853	0.341	Orifice
0.100	0.863	0.374	Orifice
0.100	0.878	0.419	Orifice
0.117	0.226	0.238	Non-Orifice
0.117	0.321	0.239	Non-Orifice
0.117	0.421	0.242	Non-Orifice
0.117	0.477	0.245	Non-Orifice
0.117	0.529	0.249	Non-Orifice
0.117	0.606	0.254	Non-Orifice
0.117	0.649	0.257	Non-Orifice
0.117	0.689	0.264	Non-Orifice
0.117	0.728	0.269	Transition Non-Orifice & Orifice
0.117	0.743	0.277	Transition Non-Orifice & Orifice
0.117	0.752	0.279	Transition Non-Orifice & Orifice
0.117	0.759	0.282	Transition Non-Orifice & Orifice
0.117	0.767	0.284	Transition Non-Orifice & Orifice
0.117	0.788	0.293	Transition Non-Orifice & Orifice
0.117	0.798	0.302	Transition Non-Orifice & Orifice
0.117	0.800	0.311	Orifice
0.117	0.803	0.321	Orifice
0.117	0.809	0.341	Orifice
0.117	0.814	0.379	Orifice
0.117	0.830	0.429	Orifice
0.135	0.238	0.259	Non-Orifice
0.135	0.334	0.260	Non-Orifice
0.135	0.412	0.264	Non-Orifice
0.135	0.473	0.266	Non-Orifice
0.135	0.527	0.269	Non-Orifice
0.135	0.575	0.276	Transition Non-Orifice & Orifice
0.135	0.614	0.283	Transition Non-Orifice & Orifice
0.135	0.628	0.285	Transition Non-Orifice & Orifice
0.135	0.629	0.287	Transition Non-Orifice & Orifice
0.135	0.643	0.289	Transition Non-Orifice & Orifice
0.135	0.671	0.298	Orifice
0.135	0.697	0.304	Orifice
0.135	0.722	0.313	Orifice
0.135	0.738	0.321	Orifice
0.135	0.743	0.331	Orifice
0.135	0.750	0.341	Orifice
0.135	0.748	0.353	Orifice
0.135	0.751	0.374	Orifice
0.135	0.764	0.412	Orifice
0.135	0.778	0.447	Orifice

Table 14. Laboratory Data for a Gate Opening of 0.30 m

Q (m^3/s)	S	h_u (m)	Gate Status
0.027	0.542	0.090	Non-Orifice
0.027	0.775	0.098	Non-Orifice
0.027	0.892	0.112	Non-Orifice
0.027	0.913	0.127	Non-Orifice
0.027	0.916	0.144	Non-Orifice
0.027	0.950	0.162	Non-Orifice
0.027	0.955	0.178	Non-Orifice
0.027	0.959	0.194	Non-Orifice
0.027	0.976	0.210	Non-Orifice
0.027	0.982	0.227	Non-Orifice
0.027	0.988	0.242	Non-Orifice
0.027	0.992	0.256	Non-Orifice
0.027	1.000	0.282	Non-Orifice
0.027	0.993	0.299	Transition Non-Orifice & Orifice
0.027	0.997	0.312	Orifice
0.027	0.994	0.333	Orifice
0.027	0.995	0.373	Orifice
0.027	0.998	0.404	Orifice
0.027	0.995	0.423	Orifice
0.035	0.595	0.104	Non-Orifice
0.035	0.789	0.114	Non-Orifice
0.035	0.948	0.194	Non-Orifice
0.035	0.965	0.202	Non-Orifice
0.035	0.971	0.210	Non-Orifice
0.035	0.978	0.226	Non-Orifice
0.035	0.975	0.242	Non-Orifice
0.035	0.985	0.261	Non-Orifice
0.035	0.993	0.276	Non-Orifice
0.035	0.986	0.291	Non-Orifice
0.035	0.987	0.298	Transition Non-Orifice & Orifice
0.035	0.993	0.300	Orifice
0.035	0.993	0.302	Orifice
0.035	0.987	0.309	Orifice
0.035	0.991	0.323	Orifice
0.035	0.991	0.348	Orifice
0.035	0.987	0.384	Orifice
0.035	0.994	0.405	Orifice
0.035	0.993	0.424	Orifice
0.046	0.315	0.123	Non-Orifice
0.046	0.539	0.124	Non-Orifice
0.046	0.637	0.127	Non-Orifice
0.046	0.732	0.131	Non-Orifice
0.046	0.760	0.138	Non-Orifice
0.046	0.812	0.144	Non-Orifice
0.046	0.822	0.152	Non-Orifice
0.046	0.855	0.159	Non-Orifice
0.046	0.880	0.167	Non-Orifice
0.046	0.903	0.175	Non-Orifice
0.046	0.913	0.184	Non-Orifice
0.046	0.916	0.192	Non-Orifice
0.046	0.925	0.201	Non-Orifice
0.046	0.937	0.207	Non-Orifice
0.046	0.942	0.224	Non-Orifice
0.046	0.962	0.239	Non-Orifice
0.046	0.965	0.255	Non-Orifice
0.046	0.982	0.282	Non-Orifice
0.046	0.980	0.303	Transition Non-Orifice & Orifice
0.046	0.985	0.344	Orifice
0.046	0.990	0.404	Orifice
0.051	0.354	0.132	Non-Orifice
0.051	0.495	0.133	Non-Orifice
0.051	0.583	0.137	Non-Orifice
0.051	0.666	0.141	Non-Orifice
0.051	0.720	0.147	Non-Orifice
0.051	0.766	0.154	Non-Orifice
0.051	0.801	0.161	Non-Orifice
0.051	0.875	0.169	Non-Orifice
0.051	0.892	0.176	Non-Orifice
0.051	0.920	0.201	Non-Orifice
0.051	0.942	0.208	Non-Orifice
0.051	0.940	0.217	Non-Orifice
0.051	0.962	0.240	Non-Orifice
0.051	0.968	0.249	Non-Orifice
0.051	0.969	0.256	Non-Orifice
0.051	0.973	0.264	Non-Orifice
0.051	0.975	0.279	Non-Orifice
0.051	0.980	0.294	Non-Orifice
0.051	0.980	0.308	Transition Non-Orifice & Orifice
0.051	0.984	0.322	Orifice
0.051	0.988	0.348	Orifice
0.051	0.988	0.410	Orifice
0.051	0.986	0.442	Orifice
0.066	0.344	0.165	Non-Orifice
0.066	0.469	0.166	Non-Orifice
0.066	0.549	0.171	Non-Orifice
0.066	0.614	0.174	Non-Orifice
0.066	0.681	0.179	Non-Orifice
0.066	0.735	0.185	Non-Orifice
0.066	0.785	0.191	Non-Orifice
0.066	0.789	0.199	Non-Orifice
0.066	0.810	0.206	Non-Orifice
0.066	0.836	0.214	Non-Orifice
0.066	0.874	0.230	Non-Orifice
0.066	0.904	0.244	Non-Orifice
0.066	0.927	0.260	Non-Orifice
0.066	0.945	0.274	Non-Orifice
0.066	0.958	0.289	Non-Orifice
0.066	0.957	0.305	Transition Non-Orifice & Orifice
0.066	0.966	0.320	Orifice
0.066	0.959	0.350	Orifice
0.066	0.964	0.391	Orifice
0.066	0.967	0.428	Orifice
0.075	0.245	0.178	Non-Orifice
0.075	0.373	0.179	Non-Orifice
0.075	0.480	0.181	Non-Orifice
0.075	0.569	0.186	Non-Orifice
0.075	0.612	0.191	Non-Orifice
0.075	0.654	0.197	Non-Orifice
0.075	0.719	0.203	Non-Orifice
0.075	0.756	0.209	Non-Orifice
0.075	0.791	0.216	Non-Orifice
0.075	0.827	0.232	Non-Orifice
0.075	0.862	0.247	Non-Orifice
0.075	0.902	0.267	Non-Orifice
0.075	0.919	0.273	Non-Orifice
0.075	0.928	0.279	Non-Orifice
0.075	0.939	0.296	Non-Orifice
0.075	0.947	0.304	Non-Orifice
0.075	0.952	0.310	Transition Non-Orifice & Orifice
0.075	0.956	0.318	Orifice
0.075	0.955	0.334	Orifice
0.075	0.953	0.364	Orifice
0.075	0.958	0.404	Orifice
0.075	0.955	0.444	Orifice

Note: Submergence equal to one corresponds to the condition where it was not possible to distinguish between upstream and downstream depths using the water manometer.

Q (m^3/s)	S	h_u (m)	Gate Status
0.100	0.236	0.215	Non-Orifice
0.100	0.287	0.215	Non-Orifice
0.100	0.398	0.218	Non-Orifice
0.100	0.481	0.222	Non-Orifice
0.100	0.541	0.225	Non-Orifice
0.100	0.601	0.231	Non-Orifice
0.100	0.656	0.236	Non-Orifice
0.100	0.698	0.242	Non-Orifice
0.100	0.730	0.249	Non-Orifice
0.100	0.763	0.254	Non-Orifice
0.100	0.816	0.266	Non-Orifice
0.100	0.842	0.272	Non-Orifice
0.100	0.861	0.280	Non-Orifice
0.100	0.864	0.288	Non-Orifice
0.100	0.872	0.297	Non-Orifice
0.100	0.885	0.304	Non-Orifice
0.100	0.897	0.311	Transition Non-Orifice & Orifice
0.100	0.908	0.327	Orifice
0.100	0.910	0.344	Orifice
0.100	0.920	0.375	Orifice
0.100	0.919	0.422	Orifice
0.117	0.226	0.238	Non-Orifice
0.117	0.321	0.239	Non-Orifice
0.117	0.421	0.242	Non-Orifice
0.117	0.477	0.245	Non-Orifice
0.117	0.529	0.249	Non-Orifice
0.117	0.606	0.254	Non-Orifice
0.117	0.649	0.257	Non-Orifice
0.117	0.689	0.264	Non-Orifice
0.117	0.729	0.270	Non-Orifice
0.117	0.753	0.276	Non-Orifice
0.117	0.800	0.290	Non-Orifice
0.117	0.841	0.303	Non-Orifice
0.117	0.861	0.318	Transition Non-Orifice & Orifice
0.117	0.874	0.325	Transition Non-Orifice & Orifice
0.117	0.880	0.334	Orifice
0.117	0.886	0.343	Orifice
0.117	0.881	0.352	Orifice
0.117	0.886	0.369	Orifice
0.117	0.883	0.403	Orifice
0.117	0.887	0.434	Orifice

Q (m^3/s)	S	h_u (m)	Gate Status
0.135	0.233	0.260	Non-Orifice
0.135	0.331	0.262	Non-Orifice
0.135	0.423	0.264	Non-Orifice
0.135	0.464	0.267	Non-Orifice
0.135	0.542	0.271	Non-Orifice
0.135	0.575	0.276	Non-Orifice
0.135	0.636	0.281	Non-Orifice
0.135	0.671	0.286	Non-Orifice
0.135	0.712	0.292	Non-Orifice
0.135	0.757	0.305	Non-Orifice
0.135	0.798	0.318	Transition Non-Orifice & Orifice
0.135	0.815	0.324	Transition Non-Orifice & Orifice
0.135	0.832	0.333	Orifice
0.135	0.839	0.341	Orifice
0.135	0.840	0.350	Orifice
0.135	0.847	0.359	Orifice
0.135	0.846	0.378	Orifice
0.135	0.850	0.413	Orifice
0.135	0.852	0.447	Orifice
0.151	0.254	0.278	Non-Orifice
0.151	0.290	0.278	Non-Orifice
0.151	0.383	0.281	Non-Orifice
0.151	0.436	0.284	Non-Orifice
0.151	0.501	0.287	Non-Orifice
0.151	0.551	0.292	Non-Orifice
0.151	0.591	0.299	Non-Orifice
0.151	0.632	0.302	Non-Orifice
0.151	0.662	0.308	Non-Orifice
0.151	0.700	0.314	Non-Orifice
0.151	0.731	0.320	Transition Non-Orifice & Orifice
0.151	0.749	0.327	Transition Non-Orifice & Orifice
0.151	0.769	0.334	Transition Non-Orifice & Orifice
0.151	0.781	0.343	Transition Non-Orifice & Orifice
0.151	0.800	0.350	Orifice
0.151	0.804	0.358	Orifice
0.151	0.809	0.378	Orifice
0.151	0.811	0.397	Orifice
0.151	0.817	0.433	Orifice
0.151	0.818	0.450	Orifice

Q (m^3/s)	S	h_u (m)	Gate Status
0.166	0.282	0.297	Non-Orifice
0.166	0.275	0.297	Non-Orifice
0.166	0.330	0.299	Non-Orifice
0.166	0.392	0.303	Non-Orifice
0.166	0.447	0.306	Non-Orifice
0.166	0.507	0.309	Non-Orifice
0.166	0.547	0.312	Non-Orifice
0.166	0.592	0.319	Non-Orifice
0.166	0.635	0.326	Transition Non-Orifice & Orifice
0.166	0.684	0.339	Transition Non-Orifice & Orifice
0.166	0.727	0.352	Transition Non-Orifice & Orifice
0.166	0.750	0.369	Orifice
0.166	0.773	0.384	Orifice
0.166	0.776	0.424	Orifice
0.166	0.775	0.444	Orifice

Table 15. Laboratory Data for a Gate Opening of 0.35 m

Q (m^3/s)	S	h_u (m)	Gate Status
0.027	0.542	0.090	Non-Orifice
0.027	0.775	0.098	Non-Orifice
0.027	0.892	0.112	Non-Orifice
0.027	0.913	0.127	Non-Orifice
0.027	0.916	0.144	Non-Orifice
0.027	0.950	0.162	Non-Orifice
0.027	0.955	0.178	Non-Orifice
0.027	0.959	0.194	Non-Orifice
0.027	0.976	0.210	Non-Orifice
0.027	0.982	0.227	Non-Orifice
0.027	0.988	0.242	Non-Orifice
0.027	0.992	0.256	Non-Orifice
0.027	1.000	0.282	Non-Orifice
0.027	1.000	0.297	Non-Orifice
0.027	1.000	0.310	Non-Orifice
0.027	1.000	0.323	Non-Orifice
0.027	1.000	0.334	Non-Orifice
0.027	1.000	0.348	Transition Non-Orifice & Orifice
0.027	0.997	0.361	Orifice
0.027	1.000	0.383	Orifice
0.027	1.000	0.410	Orifice
0.046	0.315	0.123	Non-Orifice
0.046	0.539	0.124	Non-Orifice
0.046	0.637	0.127	Non-Orifice
0.046	0.732	0.131	Non-Orifice
0.046	0.760	0.138	Non-Orifice
0.046	0.812	0.144	Non-Orifice
0.046	0.822	0.152	Non-Orifice
0.046	0.855	0.159	Non-Orifice
0.046	0.880	0.167	Non-Orifice
0.046	0.903	0.175	Non-Orifice
0.046	0.913	0.184	Non-Orifice
0.046	0.916	0.192	Non-Orifice
0.046	0.925	0.201	Non-Orifice
0.046	0.937	0.207	Non-Orifice
0.046	0.942	0.224	Non-Orifice
0.046	0.962	0.239	Non-Orifice
0.046	0.965	0.255	Non-Orifice
0.046	0.982	0.282	Non-Orifice
0.046	0.990	0.310	Non-Orifice
0.046	0.991	0.351	Transition Non-Orifice & Orifice
0.046	0.989	0.360	Orifice
0.046	0.992	0.384	Orifice
0.046	0.993	0.418	Orifice
0.046	0.993	0.448	Orifice
0.051	0.354	0.132	Non-Orifice
0.051	0.495	0.133	Non-Orifice
0.051	0.583	0.137	Non-Orifice
0.051	0.666	0.141	Non-Orifice
0.051	0.720	0.147	Non-Orifice
0.051	0.766	0.154	Non-Orifice
0.051	0.801	0.161	Non-Orifice
0.051	0.875	0.169	Non-Orifice
0.051	0.892	0.176	Non-Orifice
0.051	0.920	0.201	Non-Orifice
0.051	0.942	0.208	Non-Orifice
0.051	0.940	0.217	Non-Orifice
0.051	0.962	0.240	Non-Orifice
0.051	0.968	0.249	Non-Orifice
0.051	0.969	0.256	Non-Orifice
0.051	0.973	0.264	Non-Orifice
0.051	0.975	0.279	Non-Orifice
0.051	0.980	0.294	Non-Orifice
0.051	0.980	0.308	Non-Orifice
0.051	0.984	0.322	Non-Orifice
0.051	0.988	0.335	Non-Orifice
0.051	0.989	0.349	Transition Non-Orifice & Orifice
0.051	0.989	0.361	Orifice
0.051	0.990	0.385	Orifice
0.051	0.995	0.417	Orifice
0.051	0.995	0.437	Orifice
0.066	0.344	0.165	Non-Orifice
0.066	0.469	0.166	Non-Orifice
0.066	0.549	0.171	Non-Orifice
0.066	0.614	0.174	Non-Orifice
0.066	0.681	0.179	Non-Orifice
0.066	0.735	0.185	Non-Orifice
0.066	0.785	0.191	Non-Orifice
0.066	0.789	0.199	Non-Orifice
0.066	0.810	0.206	Non-Orifice
0.066	0.836	0.214	Non-Orifice
0.066	0.874	0.230	Non-Orifice
0.066	0.904	0.244	Non-Orifice
0.066	0.927	0.260	Non-Orifice
0.066	0.945	0.274	Non-Orifice
0.066	0.958	0.289	Non-Orifice
0.066	0.964	0.304	Non-Orifice
0.066	0.969	0.319	Non-Orifice
0.066	0.975	0.354	Transition Non-Orifice & Orifice
0.066	0.976	0.368	Orifice
0.066	0.977	0.387	Orifice
0.066	0.981	0.412	Orifice
0.066	0.979	0.436	Orifice
0.075	0.245	0.178	Non-Orifice
0.075	0.373	0.179	Non-Orifice
0.075	0.480	0.181	Non-Orifice
0.075	0.569	0.186	Non-Orifice
0.075	0.612	0.191	Non-Orifice
0.075	0.654	0.197	Non-Orifice
0.075	0.719	0.203	Non-Orifice
0.075	0.756	0.209	Non-Orifice
0.075	0.791	0.216	Non-Orifice
0.075	0.827	0.232	Non-Orifice
0.075	0.862	0.247	Non-Orifice
0.075	0.902	0.267	Non-Orifice
0.075	0.919	0.273	Non-Orifice
0.075	0.928	0.279	Non-Orifice
0.075	0.928	0.279	Non-Orifice
0.075	0.939	0.296	Non-Orifice
0.075	0.952	0.311	Non-Orifice
0.075	0.960	0.324	Non-Orifice
0.075	0.965	0.339	Non-Orifice
0.075	0.963	0.354	Transition Non-Orifice & Orifice
0.075	0.966	0.382	Orifice
0.075	0.974	0.419	Orifice

Note: Submergence equal to one corresponds to the condition where it was not possible to distinguish between upstream and downstream depths using the water manometer.

Q (m^3/s)	S	h_u (m)	Gate Status
0.100	0.236	0.215	Non-Orifice
0.100	0.287	0.215	Non-Orifice
0.100	0.398	0.218	Non-Orifice
0.100	0.481	0.222	Non-Orifice
0.100	0.541	0.225	Non-Orifice
0.100	0.601	0.231	Non-Orifice
0.100	0.656	0.236	Non-Orifice
0.100	0.698	0.242	Non-Orifice
0.100	0.730	0.249	Non-Orifice
0.100	0.763	0.254	Non-Orifice
0.100	0.816	0.266	Non-Orifice
0.100	0.842	0.272	Non-Orifice
0.100	0.861	0.280	Non-Orifice
0.100	0.864	0.288	Non-Orifice
0.100	0.872	0.297	Non-Orifice
0.100	0.885	0.304	Non-Orifice
0.100	0.906	0.318	Non-Orifice
0.100	0.922	0.332	Non-Orifice
0.100	0.936	0.346	Non-Orifice
0.100	0.938	0.356	Transition Non-Orifice & Orifice
0.100	0.939	0.364	Transition Non-Orifice & Orifice
0.100	0.941	0.372	Transition Non-Orifice & Orifice
0.100	0.948	0.386	Orifice
0.100	0.949	0.414	Orifice
0.100	0.951	0.454	Orifice
0.117	0.226	0.238	Non-Orifice
0.117	0.321	0.239	Non-Orifice
0.117	0.421	0.242	Non-Orifice
0.117	0.477	0.245	Non-Orifice
0.117	0.529	0.249	Non-Orifice
0.117	0.606	0.254	Non-Orifice
0.117	0.649	0.257	Non-Orifice
0.117	0.689	0.264	Non-Orifice
0.117	0.729	0.270	Non-Orifice
0.117	0.753	0.276	Non-Orifice

Q (m^3/s)	S	h_u (m)	Gate Status
0.117	0.800	0.290	Non-Orifice
0.117	0.841	0.303	Non-Orifice
0.117	0.852	0.311	Non-Orifice
0.117	0.874	0.325	Non-Orifice
0.117	0.894	0.339	Non-Orifice
0.117	0.914	0.362	Transition Non-Orifice & Orifice
0.117	0.916	0.369	Transition Non-Orifice & Orifice
0.117	0.920	0.377	Orifice
0.117	0.924	0.393	Orifice
0.117	0.922	0.423	Orifice
0.135	0.233	0.260	Non-Orifice
0.135	0.331	0.262	Non-Orifice
0.135	0.423	0.264	Non-Orifice
0.135	0.464	0.267	Non-Orifice
0.135	0.542	0.271	Non-Orifice
0.135	0.575	0.276	Non-Orifice
0.135	0.636	0.281	Non-Orifice
0.135	0.671	0.286	Non-Orifice
0.135	0.712	0.292	Non-Orifice
0.135	0.757	0.305	Non-Orifice
0.135	0.813	0.326	Non-Orifice
0.135	0.843	0.339	Non-Orifice
0.135	0.867	0.354	Non-Orifice
0.135	0.893	0.374	Transition Non-Orifice & Orifice
0.135	0.895	0.382	Transition Non-Orifice & Orifice
0.135	0.900	0.390	Orifice
0.135	0.897	0.408	Orifice
0.135	0.902	0.439	Orifice

Q (m^3/s)	S	h_u (m)	Gate Status
0.151	0.254	0.278	Non-Orifice
0.151	0.290	0.278	Non-Orifice
0.151	0.383	0.281	Non-Orifice
0.151	0.436	0.284	Non-Orifice
0.151	0.501	0.287	Non-Orifice
0.151	0.551	0.292	Non-Orifice
0.151	0.591	0.299	Non-Orifice
0.151	0.632	0.302	Non-Orifice
0.151	0.662	0.308	Non-Orifice
0.151	0.700	0.314	Non-Orifice
0.151	0.729	0.321	Non-Orifice
0.151	0.754	0.326	Non-Orifice
0.151	0.768	0.333	Non-Orifice
0.151	0.812	0.346	Non-Orifice
0.151	0.838	0.359	Non-Orifice
0.151	0.845	0.367	Transition Non-Orifice & Orifice
0.151	0.853	0.374	Transition Non-Orifice & Orifice
0.151	0.864	0.382	Orifice
0.151	0.879	0.414	Orifice
0.151	0.879	0.448	Orifice
0.166	0.282	0.297	Non-Orifice
0.166	0.275	0.297	Non-Orifice
0.166	0.330	0.299	Non-Orifice
0.166	0.392	0.303	Non-Orifice
0.166	0.447	0.306	Non-Orifice
0.166	0.507	0.309	Non-Orifice
0.166	0.547	0.312	Non-Orifice
0.166	0.592	0.319	Non-Orifice
0.166	0.629	0.324	Non-Orifice
0.166	0.665	0.329	Non-Orifice
0.166	0.700	0.334	Non-Orifice
0.166	0.727	0.341	Non-Orifice
0.166	0.757	0.354	Non-Orifice
0.166	0.782	0.359	Non-Orifice
0.166	0.795	0.367	Transition Non-Orifice & Orifice
0.166	0.820	0.372	Transition Non-Orifice & Orifice
0.166	0.834	0.379	Transition Non-Orifice & Orifice
0.166	0.845	0.394	Orifice
0.166	0.853	0.429	Orifice
0.166	0.852	0.447	Orifice

Appendix V. Transition Threshold Using the Submerged Non-orifice Equation

Table 16. Error Analysis Showing the Second Approach used to Define Transition Threshold using the Submerged Non-orifice Equation (Eq. 2)

		Laboratory		Traditional Equation Subm Non Orifice (Eq. 2)	
G_o (m)	Number of Points	Gate Status	Q measured (m^3/s)	Q estimated (m^3/s)	% Error
0.15	1	Non Orifice	0.066	0.066	1
	2	Transition Non-Orifice & Orifice	0.066	0.064	3
	3	Transition Non-Orifice & Orifice	0.066	0.063	5
	4	Orifice	0.066	0.063	5
	5	Orifice	0.066	0.074	-12
	6	Orifice	0.066	0.086	-30
	7	Orifice	0.066	0.098	-48
	8	Orifice	0.066	0.110	-65
	9	Orifice	0.066	0.129	-95
0.2	1	Non Orifice	0.075	0.071	5
	2	Non Orifice	0.075	0.074	1
	3	Non Orifice	0.075	0.074	1
	4	Non Orifice	0.075	0.074	1
	5	Non Orifice	0.075	0.074	1
	6	Non Orifice	0.075	0.074	1
	7	Non Orifice	0.075	0.072	3
	8	Non Orifice	0.075	0.071	4
	9	Transition Non-Orifice & Orifice	0.075	0.072	4
	10	Transition Non-Orifice & Orifice	0.075	0.072	3
	11	Orifice	0.075	0.068	8
	12	Orifice	0.075	0.070	6
	13	Orifice	0.075	0.074	1
	14	Orifice	0.075	0.079	-6
	15	Orifice	0.075	0.090	-21
	16	Orifice	0.075	0.108	-46
	17	Orifice	0.075	0.133	-78
0.25	1	Non Orifice	0.135	0.115	15
	2	Non Orifice	0.135	0.121	10
	3	Non Orifice	0.135	0.126	7
	4	Non Orifice	0.135	0.127	6
	5	Non Orifice	0.135	0.128	5
	6	Transition Non-Orifice & Orifice	0.135	0.130	4
	7	Transition Non-Orifice & Orifice	0.135	0.132	2
	8	Transition Non-Orifice & Orifice	0.135	0.132	2
	9	Transition Non-Orifice & Orifice	0.135	0.133	1
	10	Transition Non-Orifice & Orifice	0.135	0.133	1
	11	Orifice	0.135	0.135	-1
	12	Orifice	0.135	0.136	-1
	13	Orifice	0.135	0.138	-2
	14	Orifice	0.135	0.140	-4
	15	Orifice	0.135	0.144	-7
	16	Orifice	0.135	0.149	-10
	17	Orifice	0.135	0.156	-16
	18	Orifice	0.135	0.168	-24
	19	Orifice	0.135	0.187	-39
	20	Orifice	0.135	0.203	-51

		Laboratory		Traditional Equation Subm Non - Orifice (Eq. 2)	
G_o (m)	Number of Points	Gate Status	Q measured (m^3/s)	Q estimated (m^3/s)	% Error
0.3	1	Non Orifice	0.151	0.128	15
	2	Non Orifice	0.151	0.131	13
	3	Non Orifice	0.151	0.139	8
	4	Non Orifice	0.151	0.142	6
	5	Non Orifice	0.151	0.144	4
	6	Non Orifice	0.151	0.147	3
	7	Non Orifice	0.151	0.149	1
	8	Non Orifice	0.151	0.148	1
	9	Non Orifice	0.151	0.150	1
	10	Non Orifice	0.151	0.149	1
	11	Transition Non	0.151	0.148	1
	12	Transition Non	0.151	0.150	1
	13	Transition Non	0.151	0.150	0
	14	Transition Non	0.151	0.153	-2
	15	Orifice	0.151	0.153	-1
	16	Orifice	0.151	0.156	-4
	17	Orifice	0.151	0.167	-11
	18	Orifice	0.151	0.178	-18
	19	Orifice	0.151	0.199	-32
	20	Orifice	0.151	0.210	-39
0.35	1	Non Orifice	0.166	0.140	16
	2	Non Orifice	0.166	0.140	16
	3	Non Orifice	0.166	0.146	12
	4	Non Orifice	0.166	0.153	8
	5	Non Orifice	0.166	0.157	6
	6	Non Orifice	0.166	0.159	4
	7	Non Orifice	0.166	0.160	4
	8	Non Orifice	0.166	0.164	2
	9	Non Orifice	0.166	0.164	1
	10	Non Orifice	0.166	0.164	1
	11	Non Orifice	0.166	0.163	2
	12	Non Orifice	0.166	0.164	1
	13	Non Orifice	0.166	0.167	-1
	14	Non Orifice	0.166	0.165	1
	15	Transition Non	0.166	0.166	0
	16	Transition Non	0.166	0.162	2
	17	Transition Non	0.166	0.162	3
	18	Orifice	0.166	0.167	0
	19	Orifice	0.166	0.185	-11
	21	Orifice	0.166	0.197	-18

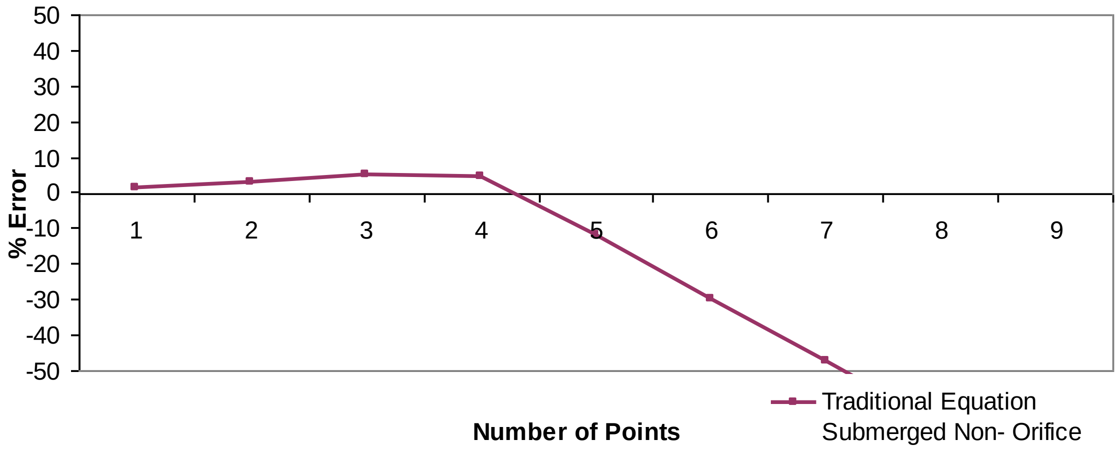

Fig. 41. Difference in error between calculated and measured discharge versus number of points measured for a discharge of 0.066 m^3/s and G_o of 0.15 m (see Table16)

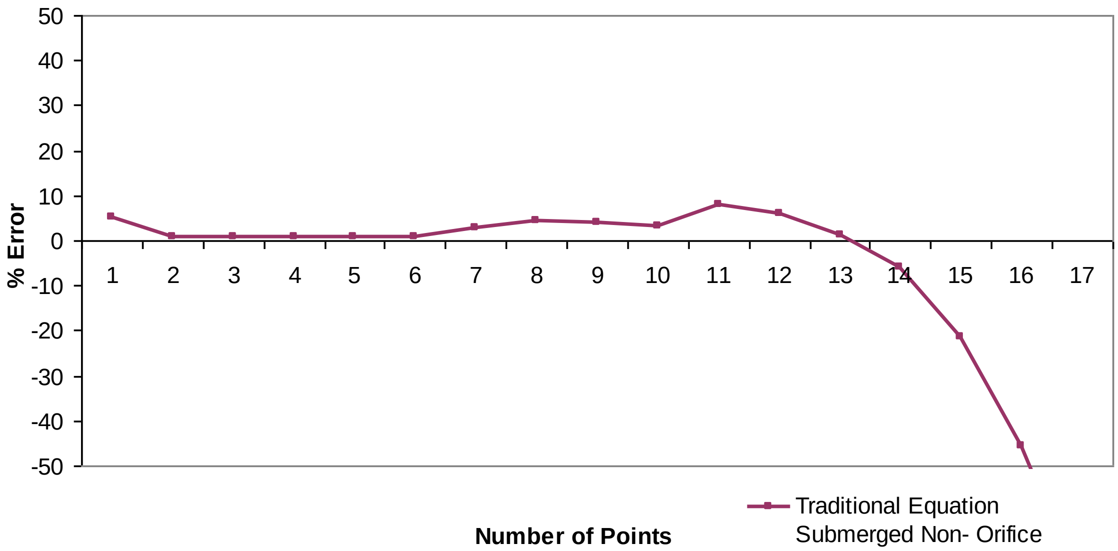

Fig. 42. Difference in error between calculated and measured discharge versus number of points measured for a discharge of 0.075 m^3/s and G_o of 0.20 m (see Table16)

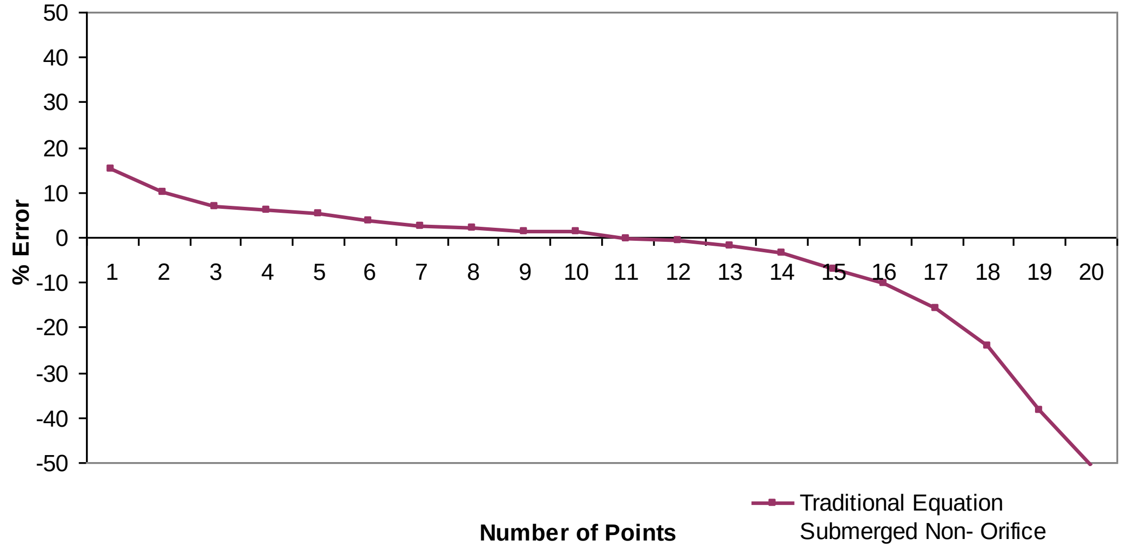

Fig. 43. Difference in error between calculated and measured discharge versus number of points measured for a discharge of 0.135 m^3/s and G_o of 0.25 m (see Table16)

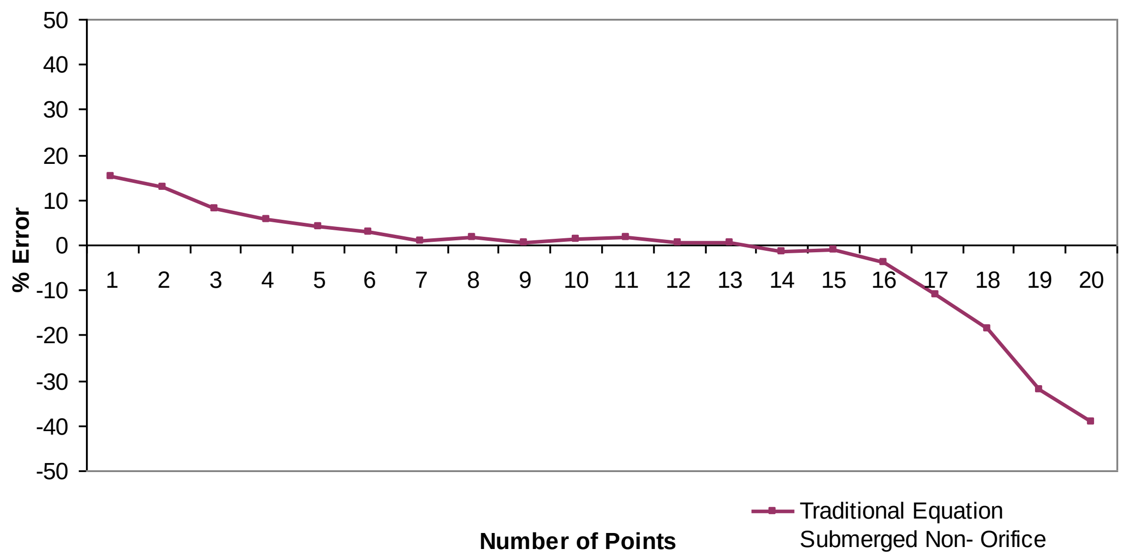

Fig. 44. Difference in error between calculated and measured discharge versus number of points measured for a discharge of 0.151 m^3/s and G_o of 0.30 m (see Table16)

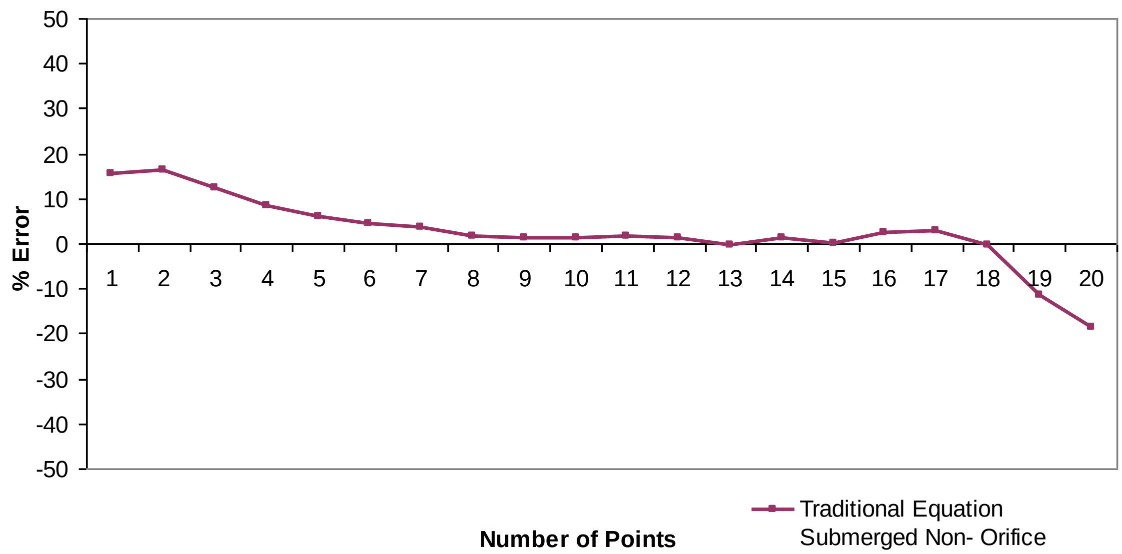

Fig. 45. Difference in error between calculated and measured discharge versus number of points measured for a discharge of 0.166 m^3/s and G_o of 0.35 m (see Table16)

Appendix VI. Sample Applications of the Regime Threshold Equations

Appendix VI

These examples of application are to determine, non-orifice and orifice transition threshold, using specific energy equation.

Example 1

For example, given: gate opening, G_o of 0.30 m ,a flow rate of 0.166 m^3/s, in a rectangular flume width upstream 0.93 m and a gate width of 0.61 m, determine the depth non-orifice transition threshold (h_{NOt}).

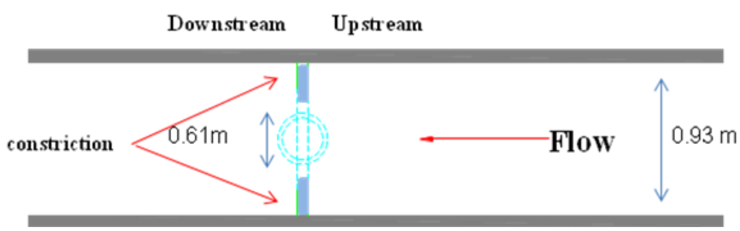

Fig.46. Plan view of the flume in the example

$$h_{NO_t} = 0.3 + \frac{0.166^2}{2(9.81)}\left(\frac{1}{(0.61*0.3)^2} - \frac{1}{(0.93*h_{NO_t})^2}\right)$$

$$h_{NO_t} = 0.326\text{m}$$

The maximum depth to define the non orifice condition is 0.326 m, greater than this depth, the water would touch the lip of the gate and the flow would be affected by the gate. Lower than 0.326 m is considered non orifice condition.

Example 2

For the same condition of example 1, determine the orifice transition threshold, h_{ot}.

$$h_{O_t} = 0.326 + \frac{0.166^2}{2(9.81)}\left(\frac{1}{(0.61*0.326)^2} - \frac{1}{(0.93*h_{O_t})^2}\right)$$

$$h_{O_t} = 0.348\text{ m}$$

The orifice condition starts to a depth of 0.348 m.

Both examples shows that it is possible to determine the limits of flow regimen, knowing G_o, flow rate and characteristic of the channel.

Appendix VII. Details of the Fitted Equation

Appendix VII

Parameters for Proposed Equations

Table 17. Parameters for the Proposed Equations

No.	Equation	r^2	SEE (m3/s)	a	b	c	d	e	f	g	h
I	$h_u = \frac{(a+bS)Q+(cS+d)}{1+(eQ+f)S+(gQ+h)Q^2}$	0.988	0.005	1.356	-1.101	-0.056	0.056	0.952	-0.997	42.563	-9.526
II	$h_u = \frac{(a+bh_d)Q+(ch_d+d)}{1+(eQ+f)h_d+(gQ+h)Q^2}$	0.985	0.005	2.163	-10.352	0.831	-0.005	-16.616	-0.439	-24.162	10.838
III	$h_u = \frac{(a+bQ)h_d+(cQ+d)}{1+(eh_d+f)Q+(gh_d+h)h_d^2}$	0.982	0.006	0.795	-12.230	2.786	-0.010	-21.245	3.069	14.982	-7.112
IV	$Q = \frac{(a+bh_d)h_u+(ch_d+d)}{1+(eh_u+f)h_d+(gh_u+h)h_u^2}$	0.991	0.004	0.417	0.093	-0.468	0.010	16.731	-7.243	-13.511	1.509
V	$Q = \frac{(a+bh_u)h_d+(ch_u+d)}{1+(eh_d+f)h_u+(gh_d+h)h_d^2}$	0.974	0.007	-0.465	-0.527	0.683	-0.005	-1.120	0.154	41.746	-19.653
VI	$Q = \frac{(a+bS)h_u+(cS+d)}{1+(eh_u+f)S+(gh_u+h)h_u^2}$	0.996	0.003	0.445	-0.431	0.009	-0.011	1.377	-1.014	7.017	-5.475

Appendix VIII. Bibliography

BIBLIOGRAPHY

Diamond W. 1989. *Practical Experiment Design for Engineers and Scientists*. Van Nostrand Reinhold. New York, NY.390 pp.

Kay, M. 1998. *Practical Hydraulics Senior Lecturer in Hydraulics and Irrigation Engineering Cranfield University*. E & FN Spon. London. 253 pp.

Ratkowsky, D. 1989. *Handbook of Nonlinear Regression Models*. Marcel Dekker Inc. New York, NY. 241 pp.

Skogerboe, G; Merkley, G. 1996. *Irrigation Maintenance and Operations Learning Process*. Water Resources Publications.Colorado. 357 pp.

USBR. 2001. *Water Measurement Manual*, Third Ed., Revised. U.S. Department of Interior, Bureau of Reclamation, Denver, CO. 327 pp.

Withers, B; Vipond, S. 1980. *Irrigation Design and Practice*. Van-Ballou Press Inc.Binghamton, N.Y. 305 pp.